Climatic and environmental controls on speleothem oxygen-isotope values

Matthew S. Lachniet*

Department of Geoscience, University of Nevada, Las Vegas, 4505 Maryland Parkway, Box 4010, Las Vegas, NV 89154, United States

ARTICLE INFO

ABSTRACT

Variations in speleothem oxygen-isotope values (δ^{18}O) result from a complicated interplay of environmental controls and processes in the ocean, atmosphere, soil zone, epikarst, and cave system. As such, the controls on speleothem δ^{18}O values are extremely complex. An understanding of the processes that control equilibrium and kinetic fractionation of oxygen isotopes in water and carbonate species is essential for the proper interpretation of speleothem δ^{18}O as paleoclimate and paleoenvironmental proxies, and is best complemented by study of site-specific cave processes such as infiltration, flow routing, drip seasonality and saturation state, and cave microclimate, among others. This review is a process-based summary of the multiple controls on δ^{18}O in the atmosphere, soil, epikarst, and speleothem calcite, illustrated with case studies. Primary controls of δ^{18}O in the atmosphere include temperature and relative humidity through their role in the multiple isotope "effects". Variability and modifications of water δ^{18}O values in the soil and epikarst zones are dominated by evaporation, mixing, and infiltration of source waters. The isotopically effective recharge into a cave system consists of those waters that participate in precipitation of $CaCO_3$, resulting in calcite deposition rates which may be biased to time periods with optimal dripwater saturation state. Recent modeling, experimental, and observational data yield insight into the significance of kinetic fractionation between dissolved carbonate phases and solid $CaCO_3$, and have implications for the 'Hendy' test. To assist interpretation of speleothem δ^{18}O time series, quantitative and semi-quantitative δ^{18}O-climate calibrations are discussed with an emphasis on some of the difficulties inherent in using modern spatial and temporal isotope gradients to interpret speleothems as paleoclimate proxy records. Finally, several case studies of globally significant speleothem paleoclimate records are discussed that show the utility of δ^{18}O to reconstruct past climate changes in regions that have been typically poorly represented in paleoclimate records, such as tropical and subtropical terrestrial locations. The new approach to speleothem paleoclimatology emphasizes climate teleconnections between regions and attribution of forcing mechanisms. Such investigations allow paleoclimatologists to infer regional to global-scale climate dynamics.

1. Introduction

In this paper, variations of oxygen isotopes in the atmosphere, the soil zone and epikarst, and finally within the cave system will be reviewed. This review is a complement to previous comprehensive multi-proxy review articles (McDermott, 2004; Fairchild et al., 2006), but differs from them in that the focus is entirely on the processes controlling variation of δ^{18}O in the Earth's climate and near surface environment and includes a quantitative treatment of δ^{18}O through these reservoirs. Because of the ubiquity of oxygen in the Earth system, the δ^{18}O value within each subsystem is controlled by a multitude of factors, with the end result of a final δ^{18}O value measured in the speleothem. As a result, the controls on

δ^{18}O of the water before reaching the drip and cave are numerous and complex.

The use of stable oxygen-isotope (δ^{18}O) values in speleothems as a paleoclimate proxy was begun in the 1960s and 1970s (Broecker et al., 1960; Hendy and Wilson, 1968; Duplessy et al., 1970; Emiliani, 1971; Hendy, 1971). Their use as a terrestrial alternative to marine sediment cores was bolstered by the observation that cave environments are quite stable and should reflect the regional mean annual temperature (Poulson and White, 1969). Under equilibrium conditions, the δ^{18}O value of speleothem carbonate is related to just two variables: the δ^{18}O value of the drip water, and the cave temperature through its control on equilibrium fractionation between water and calcite (Hendy, 1971; Kim and O'Neil, 1997; Kim et al., 2007). Despite this apparent simplicity however, variations of δ^{18}O in the global water cycle (Rozanski et al., 1993; Gat, 1996) related to several isotope effects are commonly larger in magnitude than those associated with the temperature-dependent fractionation

* Tel.: +1 702 895 4388; fax: +1 702 895 4064.
E-mail address: matthew.lachniet@unlv.edu

between water and calcite, and are therefore likely to dominate the speleothem $\delta^{18}O$ signal. Although many of the difficulties of using speleothems as a paleotemperature proxy were not initially recognized, the scientific understanding has since evolved to reveal many of the intricacies of oxygen in the hydrologic cycle, in the soil zone and epikarst, and in the cave environment. This additional knowledge has also revealed many of the challenges inherent in speleothem paleoclimatology, because multiple processes may obscure or efface the original climatic signal in speleothem $\delta^{18}O$ values.

Recent advances in understanding the climatic controls on $\delta^{18}O$ in the atmosphere and cave environment have propelled speleothems to the forefront of paleoclimatology. Analytical advances have fostered this development for two main reasons: speleothems may be dated precisely with high-precision U-series methods (Edwards et al., 1987; Richards and Dorale, 2003), and rapid automated analysis for microgram sized carbonate powders allows very high resolution time series (Wurster et al., 1999; Spötl and Mattey, 2006; Treble et al., 2007). A new emphasis on global climate teleconnections from speleothem records (Wang et al., 2001, 2004; Yuan et al., 2004; Cruz et al., 2005a; Cheng et al., 2006; Shakun et al., 2007) has replaced attempts to constrain absolute paleotemperature (Duplessy et al., 1970; Emiliani, 1971), allowing the scientific community to place global climate changes on a firm chronological and climate dynamical footing. In many cases, speleothem records may provide climate records (e.g. the China and Brazil monsoon records, and the Devils Hole record (Winograd et al., 1992; Cruz et al., 2005a; Wang et al., 2001, 2004)) that rival those obtained from marine sediment and ice cores, which usually cannot be radiometrically dated beyond the limit of the ^{14}C method ($\sim$45 ka; ka $=$ thousands of years before present). However, the $\delta^{18}O$ signal preserved in speleothems is site-specific and complicated by numerous phase changes and possible kinetic isotope effects, such that background studies on local and regional hydrology and climatology are required to interpret more confidently the paleoclimatic signal (Darling, 2004; Cruz et al., 2005b; Baldini et al., 2006; Cobb et al., 2007; McDonald et al., 2007; Mattey et al., 2008).

The primary controls on $\delta^{18}O$ relevant to speleothem studies are indicated schematically in Fig. 1, and detailed in the text. For further details on stable isotope geochemistry, the reader is referred to valuable textbooks (Clark and Fritz, 1997; Faure and Mensing, 2005; Sharp, 2007) and previous comprehensive reviews of the paleoclimatic interpretation of multi-proxy speleothem data (Schwarcz, 1986; Gascoyne, 1992; Richards and Dorale, 2003; McDermott, 2004; Fairchild et al., 2006).

1.1. Definitions, standards, and notation

The stable isotopes of oxygen of interest are ^{18}O and ^{16}O, and their variations are measured by a mass spectrometer relative to a standard, and expressed in "delta" (δ) notation (Sharp, 2007)

$$\delta^{18}O = \left(\frac{^{18}O/^{16}O_{sample} - {}^{18}O/^{16}O_{standard}}{^{18}O/^{16}O_{standard}} \right) \times 1000 \qquad (1)$$

where the standard for carbonates is Pee Dee Belemnite (PDB) (Craig, 1957), and that for waters (and carbonates) is Standard Mean Ocean Water (SMOW). More recently standards have been defined accompanied by the prefix "Vienna" or VSMOW (Gonfiantini, 1978) and VPDB to account for the exhaustion of the original standard materials (Coplen, 1995a, 1996). The original PDB and SMOW standard designations have been suggested to be discontinued (Coplen, 1995b) though this has been deemed unnecessary by others (Sharp, 2007). The isotopic ratios are expressed in ‰ "per mil" or parts per thousand notation (Sharp, 2007). The $\delta^{18}O$ value of both PDB and SMOW is defined as 0.0‰ (Coplen, 1996), and hence variations in $^{18}O/^{16}O$ ratios are expressed as differences relative to the standards. The relationship between the two scales can be expressed as (Coplen et al., 1983; Clark and Fritz, 1997; Sharp, 2007):
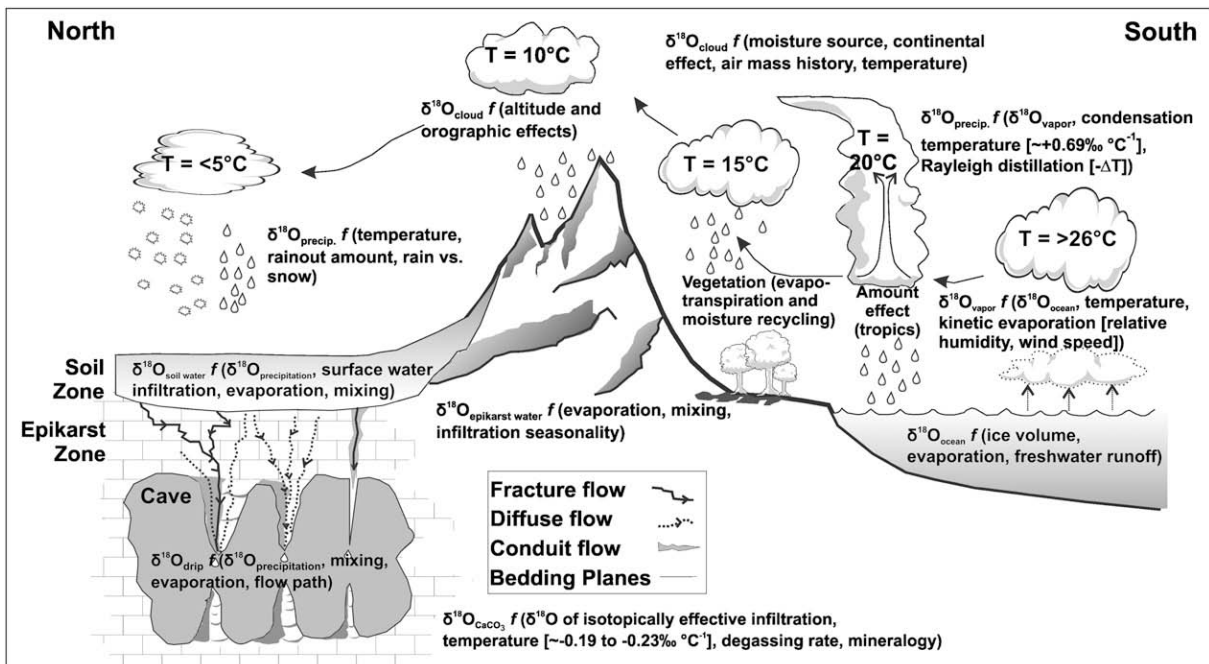

Fig. 1. Diagram illustrating the primary processes related to $\delta^{18}O$ variations relevant to speleothem paleoclimatology. The dominant controls are based on variations in temperature and relative humidity which influence the $\delta^{18}O$ values through the various processes and phase changes in the ocean, atmosphere, hydrosphere, soil and epikarst zones, and finally in speleothem $CaCO_3$. See text for additional details. In the figure f indicates it is a function of listed variables.

$$\delta^{18}O_{SMOW} = 1.03091(\delta^{18}O_{PDB}) + 30.91 \tag{2}$$

$$\delta^{18}O_{PDB} = 0.97002(\delta^{18}O_{VSMOW}) - 29.98 \tag{3}$$

When a sample has higher $\delta^{18}O$ values relative to another sample, it may be said to be "enriched" in ^{18}O or "heavier", and vice versa. For further details and rectification of common mistakes regarding verbal and written usage of the δ-‰ notation consult the excellent book by Sharp (2007).

2. $\delta^{18}O$ in the hydrologic cycle

2.1. Equilibrium and kinetic fractionation

The evolution of oxygen isotopes will be traced through the hydrologic cycle, beginning with the ocean surface, evaporation, and finally condensation of atmospheric vapor. The controls on $\delta^{18}O$ values of water in the hydrologic cycle are controlled by numerous processes associated with phase changes, for example, ocean water → vapor → liquid, etc. (Dansgaard, 1954; Craig and Gordon, 1965). During these phase changes, variations in the stable isotopic content arise due to both equilibrium and kinetic processes (Dansgaard, 1964; Craig and Gordon, 1965; Rozanski et al., 1993; Gat, 1996; Clark and Fritz, 1997). Fractionation is the process by which one isotope is favored over the other during a phase change (e.g. liquid evaporating to vapor, or precipitation of $CaCO_3$ from dissolved bicarbonate in drip waters) and is defined by

$$\alpha_{A-B} = R_A/R_B \tag{4}$$

where α is the equilibrium fractionation and R is the isotopic ratio (e.g. $^{18}O/^{16}O$) between substances A and B (Sharp, 2007). Fractionations may be either equilibrium or kinetic, the latter representing disequilibrium conditions that may obscure the original climatic signal, and result in the pronounced variations observable in $\delta^{18}O$ values. Instead of a simple ratio, fractionations are typically expressed in the form of $1000\ln\alpha$ for ease of communication because the value is more comparable to the ‰ notation.

The initial control on the $\delta^{18}O$ value of water in the hydrological cycle is the $\delta^{18}O$ value of the ocean, where the bulk of the Earth's

evaporation takes place (Dansgaard, 1964; Craig and Gordon, 1965). Spatial observations of ocean surface $\delta^{18}O$ are sparse, so gridded and smoothed estimations were produced using $\delta^{18}O$/salinity and water mass tracer proxies (LeGrande and Schmidt, 2006), shown in Fig. 2. Locally, ocean $\delta^{18}O$ values are related to salinity, which is influenced by evaporation (increases $\delta^{18}O$ values up to a few ‰), precipitation over the ocean, sea ice melt, ocean and atmospheric circulation, and freshwater runoff (decreases $\delta^{18}O$ values by several ‰). Ocean $\delta^{18}O$ values are thus sensitive to proximity to river discharge (e.g. the Amazon and Mississippi Rivers) and zones of high evaporation, such as in the Mediterranean Ocean and the subtropical North Atlantic (Dansgaard, 1954, 1964; LeGrande and Schmidt, 2006). Salinity contrasts between ocean basins may be sustained by atmospheric transport of evaporated water outside of a basin, as for the Caribbean Sea (enriched due to evaporation and removal of freshwater) to the Pacific Ocean (input of freshwater as rainfall) (Zaucker and Broecker, 1992; Schmidt et al., 2007).

During ocean evaporation, equilibrium fractionation results in less ^{18}O incorporated into the vapor than originally present in sea water, thus vapor has lower $\delta^{18}O$ values than the ocean. The equilibrium fractionation between liquid and vapor can be calculated by (Clark and Fritz, 1997):

$$1000\ln\alpha_{liquid-vapor} = 1.137\left(10^6/T_k^2\right) - 0.4156\left(10^3/T_k\right) - 2.0667 \tag{5}$$

where T is in Kelvin, and refers to the temperature of the phase change. At 25 °C (298 K), the equilibrium fractionation from ocean water to vapor is 9.34‰. Thus, vapor forming from evaporation of ocean water ($\delta^{18}O = 0.0$‰) will have a $\delta^{18}O$ value of -9.34‰ SMOW.

Additionally, there is a kinetic fractionation if the evaporation into the atmosphere from the ocean happens under relative humidity of less than 100%. The kinetic fractionation associated with liquid water evaporation may be estimated by

$$\Delta\varepsilon^{18}O_{liquid-vapor} = 14.2(1-h)‰ \tag{6}$$

where $\Delta\varepsilon^{18}O_{liquid-vapor}$ is the kinetic fractionation between the liquid and vapor, and h is the relative humidity (Gonfiantini, 1986;

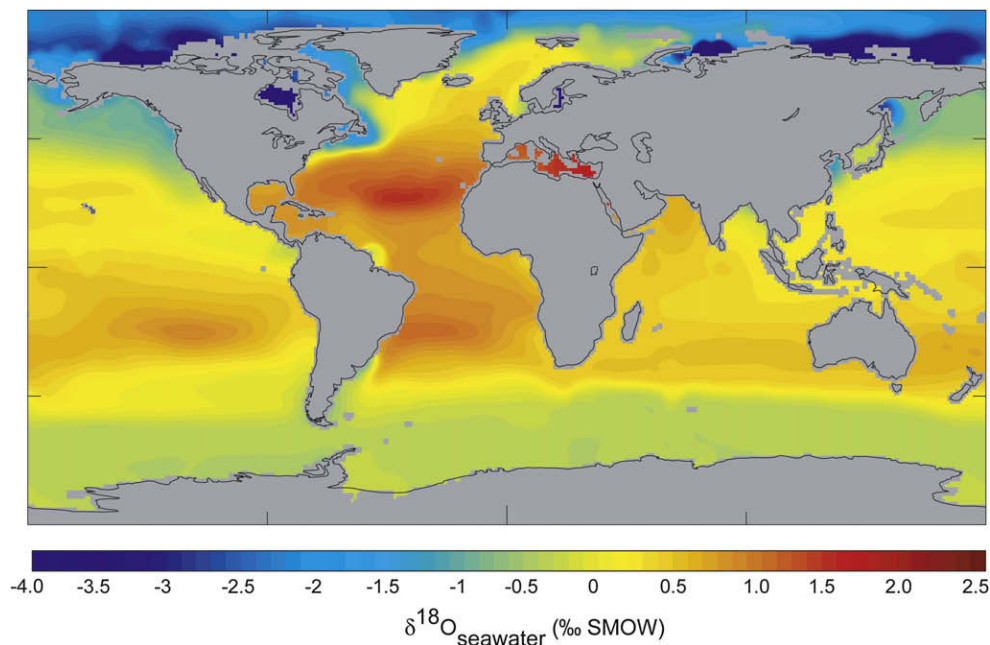**Fig. 2.** Gridded $\delta^{18}O$ of the ocean, from LeGrande and Schmidt (2006). Maximum $\delta^{18}O$ values are found in the evaporative subtropical zones, whereas low $\delta^{18}O$ values are associated with surface water input. The $\delta^{18}O$ values of regional precipitation and cave drips will thus vary by moisture source and the environmental controls on ocean evaporation.

Clark and Fritz, 1997). For example, $\Delta\varepsilon^{18}O_{liquid-vapor}$ associated with evaporation at a relative humidity of 85% is 2.13‰. Thus, the combined fractionation between liquid and vapor is $9.34 + 2.13 = 11.47$‰, and the vapor formed from SMOW has a $\delta^{18}O$ value of -11.47‰.

Following evaporation, the moisture is transported as atmospheric vapor, where it may form clouds that produce precipitation. In contrast to evaporation, condensation of vapor to liquid is an equilibrium process (Eq. (5)). Because ^{18}O is preferentially incorporated into the more condensed phase (liquid), the rain $\delta^{18}O$ value will be higher than the remaining vapor, which will itself decrease slightly because of the preferential removal of ^{18}O. To condense more moisture the cloud temperature must decrease, and this may take place due to orographic lifting, convection, or frontal cooling. The quantity of moisture condensed, and hence the remaining cloud vapor's $\delta^{18}O$ value, is thus controlled primarily by the total drop in temperature and the mass of moisture vapor in the cloud (Dansgaard, 1954, 1964; Alley and Cuffey, 2001). This process of progressive condensation and lowering of precipitation $\delta^{18}O$ value is called Rayleigh distillation, and the $\delta^{18}O$ value of vapor can be approximated by

$$\delta^{18}O_{vapor(f)} \approx \delta_0^{18}O_{vapor} + \varepsilon^{18}O_{liquid-vapor} \times \ln f \qquad (7)$$

where $\delta_0^{18}O_{vapor}$ is the initial $\delta^{18}O$ value of the vapor, f is the fraction of moisture remaining in the cloud, and $\varepsilon^{18}O_{liquid-vapor}$ is the equilibrium fractionation between vapor and liquid, which is nearly identical to the fractionation $1000\ln\alpha$ (Clark and Fritz, 1997; Sharp, 2007). The $\delta^{18}O$ value of the rain at fraction remaining (f) is then given by

$$\delta^{18}O_{rain(f)} \approx {}^{18}O_{vapor(f)} + \varepsilon^{18}O_{liquid-vapor(T)} \qquad (8)$$

at the given temperature (T). Following the example, the first rain to fall ($f = 0.95$; RH = 85%) at $T = 25°$ is $\delta^{18}O = -2.61$‰. Progressive distillation of the air mass, forced by decreasing temperature, will result in decreasing $\delta^{18}O$ values as the fraction of water remaining in the air mass decreases (Fig. 3).

2.2. Water lines

The linear correlation of $\delta^{18}O$ and δD values in global precipitation defines the global meteoric water line (GMWL). The GMWL (Fig. 4) was originally defined as $\delta D = 8 \times \delta^{18}O + 10$ (Dansgaard,

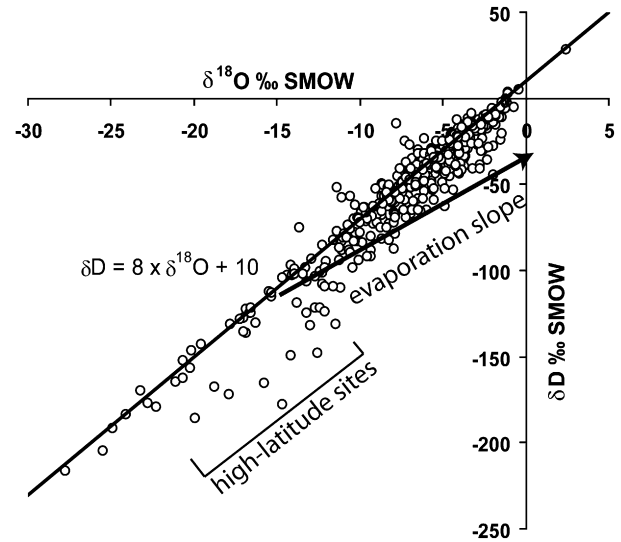**Fig. 4.** $\delta^{18}O$ and δD for stations reported in the GNIP database, shown together with the Global Meteoric Water Line (IAEA/WMO, 2004). Data plotted are from long-term weighted $\delta^{18}O$ and δD means of the GNIP stations. Locations with low deuterium intercept values (below GMWL) may arise from raindrop evaporation (for stations with high δ values) or by evaporation at high-humidity in high-latitude regions (for stations with low δ values). See text for additional details.

1964), and a more comprehensive analysis indicates $\delta D = (8.20 \pm 0.07) \times \delta^{18}O + (11.27 \pm 0.65)$ for weighted mean annual precipitation (Rozanski et al., 1993). Because both oxygen and hydrogen isotopes respond to the same isotopic processes, they are highly correlated with a slope of ~ 8, which is determined by the ratio of the $\delta D/\delta^{18}O$ equilibrium fractionation factors (Sharp, 2007). The intercept of a line with a slope of eight ($d_x = \delta D - 8 \times \delta^{18}O$) through individual isotope measurements is called the deuterium excess, and is largely determined by kinetic effects during evaporation of sea water (Dansgaard, 1964; Merlivat and Jouzel, 1979). In contrast to equilibrium fractionation, if the waters are evaporated at relative humidity less than saturation, both $\delta^{18}O$ and δD values will increase in the remaining water, plotting to the right of the GMWL with slopes of <8 (Gat, 1996). In small liquid reservoirs, such as lakes, rivers, or soil moisture, the $\delta^{18}O$ and δD values of the remaining water will significantly increase and will plot to the right of the GMWL on slopes of less

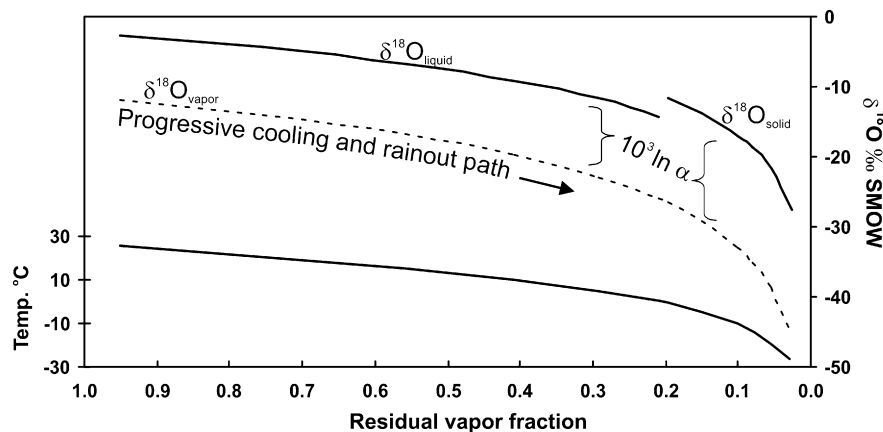**Fig. 3.** Simple Rayleigh distillation of rainfall and the change in the $\delta^{18}O$ value of water vapor, rain, and snow, as a function of decreasing temperature. Note there is a separate equilibrium fractionation for snow (see Clark and Fritz, 1997). The progressive cooling and rainout path is a result of the altitude, latitude, and orographic effects, all of which cause $\delta^{18}O$ values to decrease as rainout continues. Plot was constructed for $\delta^{18}O$ ocean of 0.0‰, evaporation at relative humidity of 85%, an initial 95% fraction of vapor remaining in cloud, and initial temperature of 25 °C.

than 8. In the ocean, the large reservoir size effectively limits the [18]O and ^{2}H enrichment of the liquid, except on long time scales associated with ice volume changes on land (discussed below). Vapor and condensation produced under very low relative humidity and high evaporation, to maintain mass balance, will then plot to the left of the GMWL, and have high deuterium excess values. Because condensation is an equilibrium process, the d_x of precipitation is inherited from the d_x of the vapor. In contrast, some high-latitude sites are characterized by water with low δ and deuterium excess values (Fig. 4) (Rozanski et al., 1993; Werner et al., 2001), which is related to the high relative humidity at the cold evaporative ocean sources (Craig and Gordon, 1965). Thus, air masses with unique deuterium intercept values may be finger-printed to a particular source regions, such as high deuterium excess values in the Mediterranean region and low values in the high-latitude regions (Rozanski et al., 1993; Bar-Matthews et al., 1996).

For speleothem studies, the local meteoric water line (LMWL) should be established by isotope measurements of precipitation for the region. The LMWL may differ from the GMWL through changes in the slope and the deuterium intercept. Slopes of LMWLs range from ∼8 to ∼5, the latter being associated with evaporative environments and lower deuterium excess values (Rozanski et al., 1993; Clark and Fritz, 1997). Establishing an LMWL is crucial to speleothem paleoclimate studies because it allows the evaluation of soil and/or drip water evaporation relative to precipitation, constraining the seasonal precipitation contribution to drip waters (Mattey et al., 2008), and to estimate moisture recycling. LMWLs have been adequately constrained in some locations via repeated and long-term analysis of precipitation δ values, commonly at those stations in the IAEA Global Network for Isotopes in Precipitation (GNIP) (IAEA/WMO, 2004). In other regions, measurement of δ values of surface and tap waters may be used as a guide (Dansgaard, 1954; Bowen et al., 2007) provided the waters have not been exposed to evaporative conditions. A local surface water line (SWL) (Kendall and Coplen, 2001) determined by δ measurements of non-evaporative rivers and groundwater may be a good approximation of the LMWL in humid regions. For example, SWLs defined by measurement of δD and $\delta^{18}O$ in rivers from the humid tropics, are $7.6 \times \delta^{18}O + 10.5$ in Costa Rica, $\delta D = 7.6 \times \delta^{18}O + 10.1$ in Panama,

and $8.2 \times \delta^{18}O + 10.9$ in Guatemala, the former two being statistically identical to MWLs (Lachniet and Patterson, 2006). The advantage of using surface waters as a proxy for meteoric waters is that samples are relatively easy to collect, and spatial sampling may also allow more precise evaluation of the geographic controls on isotopic effects (Kendall and Coplen, 2001). A disadvantage is that in non-humid regions, the δ values of the surface waters are very likely compromised by evaporation effects.

2.3. Isotope effects and air mass history

The removal of moisture from an air mass during Rayleigh distillation is temperature-dependent, because condensation of vapor requires cooling of the air mass, and because of the equilibrium fractionation during condensation (Dansgaard, 1964). The amount of moisture condensed from the cloud is thus proportional to the drop in temperature (Dansgaard, 1954, 1964). The cooling of the air parcel may arise from several processes, such as orographic lifting, advection into regions of lower temperature, convection, convergence, or frontal lifting, such that two different air masses originating from the same source may have unique rainout histories and different $\delta^{18}O$ values (Rozanski et al., 1993). The combination of the various isotope effects (Dansgaard, 1964; Rozanski et al., 1993) results in consistent and spatially coherent variation in precipitation $\delta^{18}O$ values (Bowen and Wilkinson, 2002; Bowen, 2008) that are primarily related to latitude, altitude, and moisture source. Based on IAEA station data and interpolation, the global distribution of $\delta^{18}O$ in precipitation is shown in Fig. 5 (Bowen and Wilkinson, 2002). Highest $\delta^{18}O$ values are located in the tropics and subtropics, whereas lowest values are found at high latitudes and altitudes, such as in the arctic, Antarctic, and Tibetan plateau. Of note is the fact that the magnitude of spatial $\delta^{18}O$ variations is an order of magnitude larger in the atmosphere than in the ocean (see Fig. 2), showing a stronger control of atmospheric processes on precipitation $\delta^{18}O$ values.

The temperature effect is the observed positive correlation between mean annual temperature (MAT) at-a-site and the mean $\delta^{18}O$ value of precipitation ($d\delta^{18}O_p/dT$) (Dansgaard, 1964; Fricke and O'Neill, 1999). The global relationship has been expressed as (Dansgaard, 1964):
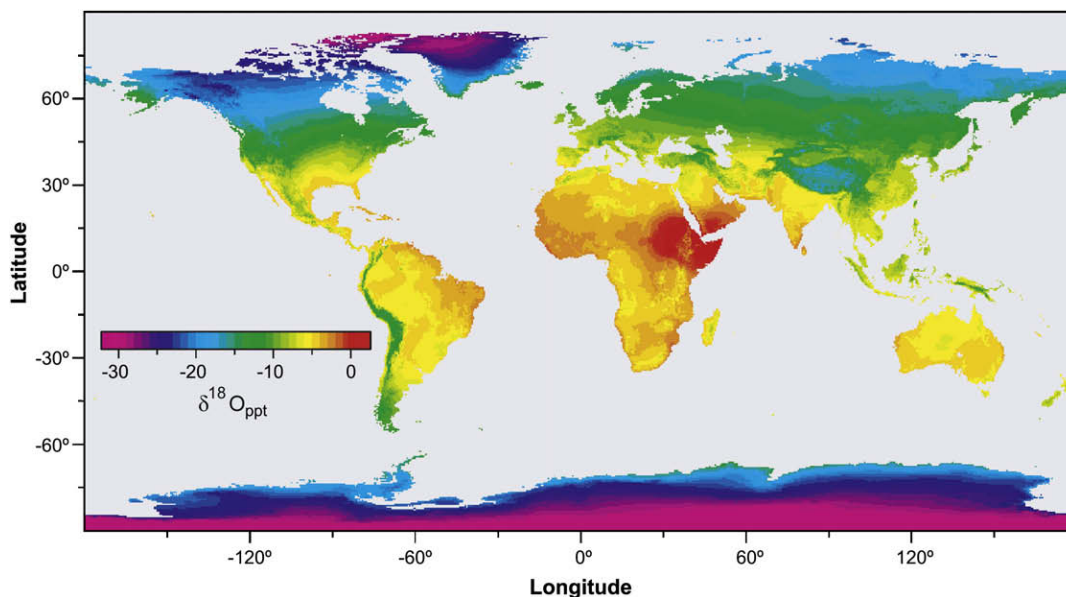

Fig. 5. Global distribution of mean annual $\delta^{18}O$ interpolated from GNIP stations shows spatial variation (Bowen and Wilkinson, 2002). $\delta^{18}O$ values decrease from low to high latitudes and altitudes, after the moisture sources have experienced significant Rayleigh distillation due to decreasing temperatures along the advection paths.

$$\delta^{18}O = 0.69(MAT) - 13.6\text{‰ SMOW} \qquad (9)$$

which is valid for middle to high latitudes. Observations (Fricke and O'Neill, 1999; Alley and Cuffey, 2001) and modeling (Jouzel et al., 1997; Schmidt et al., 2007) have indicated that the slope of the $d\delta^{18}O_p/dT$ relationship is non-linear and may vary substantially over time and space for many regions (Dansgaard, 1964; Rozanski et al., 1993), ranging from $+0.17$‰ to $+0.9$‰ $°C^{-1}$. For example, multi-proxy reconstructions of temperature over Greenland from ice cores reveal slopes that vary from 0.38‰ $°C^{-1}$ based on nitrogen and argon isotope variations in trapped air bubbles (Severinghaus and Brook, 1999) to the modern observed spatial gradient of 0.67‰ $°C^{-1}$ (Johnsen et al., 2001). Further variation of the $d\delta^{18}O_p/dT$ slope over time may be the result of changes in the seasonality of precipitation (Denton et al., 2005) and/or changes in moisture source (Charles et al., 1994). Spatial and temporal $d\delta^{18}O_p/dT$ relationships may give concordant results if $\delta^{18}O$ is correlated to the temperature of the precipitation events instead of some temporal mean (Kohn and Welker, 2005). Thus it becomes apparent that the condensation temperature is a more important control on $\delta^{18}O$ values than some statistical surface temperature mean, with the implication that proxy records such as ice cores and speleothems will be biased toward the climatic conditions associated with precipitation events.

The temperature effect has been documented to exert a strong control on the $\delta^{18}O$ values of rainfall such as Kentucky, USA (Harmon, 1979), where the gradient is 0.38‰ $°C^{-1}$, and of cave seepage waters in Israel (Ayalon et al., 1998). The temperature effect on precipitation $\delta^{18}O$ values is also manifested on a seasonal basis. $\delta^{18}O$ values are typically lower in the winter and higher in the summer. In most cases, this is due primarily to the temperature-dependent equilibrium fractionation, but also to variations in the moisture source (discussed below). The seasonal cycle generally varies by a few ‰ in the low latitudes up to 15‰ in high-latitude regions (Rozanski et al., 1993; Clark and Fritz, 1997), and may have been enhanced during past glacial periods (Denton et al., 2005).

The altitude effect is the observed decrease in $\delta^{18}O$ values with an increase in altitude, relating to the decrease in MAT with elevation (Clark and Fritz, 1997) along the local environmental lapse rate (typically of -5 to -6 $°C$ km^{-1}). The altitude effect is associated with both the decreasing temperatures of condensation and to the progressive Rayleigh distillation as the air mass is lifted over an orographic barrier. A typical range for the altitude effect is -2 to -3‰ $\delta^{18}O$ km^{-1} (Gonfiantini et al., 2001; Poage and Chamberlain, 2001; Fleitmann et al., 2004; Lachniet and Patterson, 2006). Because of the decrease in $\delta^{18}O$ values with altitude, authigenic oxygen-bearing mineral phases may be utilized as paleo-altimetry proxy records (Rowley et al., 2001; Blisniuk and Stern, 2005) on geologic time scales. Orographic distillation of air masses as they traverse a high mountain range may result in a pronounced lee-side "isotopic rain shadow" (Blisniuk and Stern, 2005).

The continental effect describes the decrease in water $\delta^{18}O$ values with distance from the ocean (Dansgaard, 1964; Rozanski et al., 1993; Clark and Fritz, 1997), and is present in both high-latitude (Ingraham and Taylor, 1991; Kendall and Coplen, 2001; Bowen and Wilkinson, 2002) and low-latitude regions (Gat and Matsui, 1991; Njitchoua et al., 1999; Lachniet and Patterson, 2006). The continental effect is a manifestation of progressive cooling and rainout of an air mass as it traverses a continent. The continental effect may be counteracted by contribution of high $\delta^{18}O$ recycled continental moisture back to the atmosphere from evaporation of soil water, lakes, and rivers (Koster et al., 1993). Plant transpiration also recycles moisture back to the atmosphere but is non-fractionating (Gat et al., 1994). As the $\delta^{18}O$ value of the recycled moisture is similar to the $\delta^{18}O$ value of the original rainfall, the net

result is a decrease in $\delta^{18}O$/distance gradients along an advection path. A notable example of moisture recycling is evident in the Amazon Basin of South America which is characterized by a very small spatial gradient in $\delta^{18}O$, and high deuterium excess values of rainfall suggest evaporation of a terrestrial moisture source (Salati et al., 1979; Gat and Matsui, 1991). Similar evidence for moisture recycling has been inferred from isotopic data for mid-western North America (Gat et al., 1994; Machavaram and Krishnamurthy, 1995), the western United States (Ingraham and Taylor, 1991), Africa (Njitchoua et al., 1999; Taupin et al., 2000), and Central America (Lachniet and Patterson, 2002).

The amount effect is the observed decrease in rainfall δ values with increased rainfall amount ($d\delta^{18}O_p/dP$) (Dansgaard, 1964; Rozanski et al., 1993; Bony et al., 2008; Risi et al., 2008), and is dominant in tropical regions where deep vertical convection is common. Such conditions are also present in tropical cyclones (Lawrence and Gedzelman, 1996), thus allowing some possibility for reconstruction of paleotempestology using speleothems (Lawrence, 1998; Frappier et al., 2007). Convection and lifting within an air parcel results from both atmospheric heating and in the equatorial zone by trade wind convergence within the intertropical convergence zone (ITCZ). Deep convection is promoted where sea surface temperatures are >27.5 $°C$ (Graham and Barnett, 1987). The amount effect has been well documented at individual tropical stations (at-a-site) (Dansgaard, 1964; Rozanski et al., 1993), but may also occur in the extratropics (Bar-Matthews et al., 2003; Treble et al., 2005a). The magnitude of the at-a-site amount effect is not constant, because it depends on the initial mass of water vapor in the air parcel, the sea surface temperature and cloud microclimate dynamics (Risi et al., 2008), as well as the amount of cooling related to the depth of convection. In Panama (Lachniet and Patterson, 2006), a humid tropical region within the heart of the ITCZ, averaged monthly $\delta^{18}O$ values are inversely correlated (Fig. 6) to rainfall amount (-2.85‰/100 mm rain; $r = -0.89$), and weight-averaged annual $\delta^{18}O$ values show a similar inverse relationship ($r = -0.66$). The amount effect is also affected by raindrop evaporation during periods of sparse rains (Dansgaard, 1964; Risi et al., 2008) when the
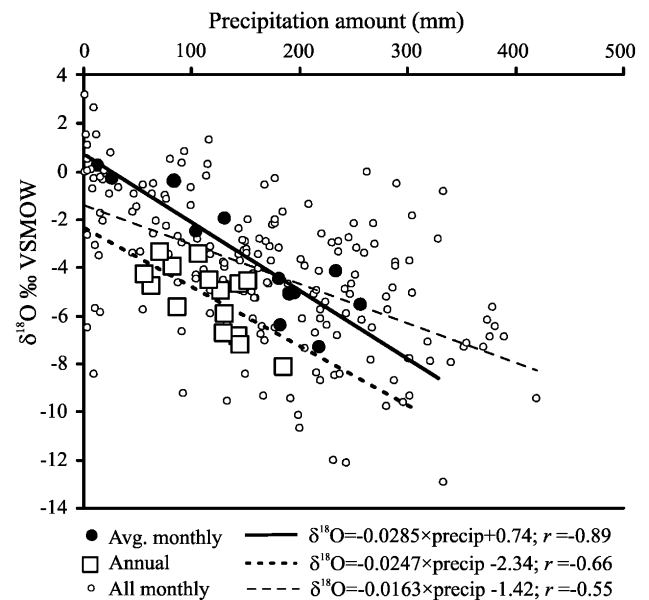

Fig. 6. The amount effect in rainfall from Panama for monthly averages (filled circles), all months (open circles), and annual $\delta^{18}O$ values with mean annual precipitation divided by 12 for plotting with monthly data (open squares). The amount effect gradient is -1.6 to -2.85‰ per 100 mm of monthly rain. From Lachniet and Patterson (2006).

relative humidity is low and is thus not a purely equilibrium process. The amount effect has also been demonstrated in the $\delta^{18}O$ values of rainfall in Barbados (Jones et al., 2000), where the gradient is -2.2 to $-2.75\permil/100$ mm of monthly rain, and in southern Oman, where seasonal rainfall $\delta^{18}O$ values vary by $\sim 2\permil$ as a function of rainfall amount (Fleitmann et al., 2004). In some regions the amount effect does not appear to be strongly manifested on a spatial basis within a region (between sites) and may even have a weak positive correlation that contrasts with the strong negative temporal correlation (Aggarwal et al., 2004; Lachniet et al., 2007). The between site $\delta^{18}O$ variability is best explained by controls of regional atmospheric circulation which integrates rainout amount along the moisture trajectory (Sturm et al., 2008).

The source effect is the observation that air masses derived from different moisture sources have distinct $\delta^{18}O$ values (Rozanski et al., 1993; Clark and Fritz, 1997; Cole et al., 1999; Friedman et al., 2002). The source effect arises from varying air mass histories and temperature of the moisture source and the regional differences in the $\delta^{18}O$ values of the ocean (LeGrande and Schmidt, 2006). In the mid-continental United States, air masses originated from the nearby Gulf of Mexico have higher $\delta^{18}O$ values than the far-traveled air masses originating from the Pacific and Arctic Oceans (Clark and Fritz, 1997; Denniston et al., 1999). In southern Brazil, precipitation and cave drip water $\delta^{18}O$ values indicate a strong source effect, with far-traveled tropical moisture having lower $\delta^{18}O$ values than more proximal subtropical Atlantic-sourced moisture (Cruz et al., 2005b; Sturm et al., 2008). Stable isotopes have also been used to constrain mixing of separate moisture sources, as over northern India which contains a mixture of both Bay of Bengal and Arabian Sea moisture (Sengupta and Sarkar, 2006), in the American southwest to constrain moisture derived from the Pacific Ocean, Gulf of Mexico, and Gulf of California (Friedman et al., 2002; Strong et al., 2007), and in southeast Asia (Araguás-Araguás et al., 1998; Aggarwal et al., 2004). Deuterium excess has also proved a good indicator of moisture source in the Mediterranean region, with Atlantic-sourced waters typically have deuterium excess values of $\sim +10\permil$, whereas Mediterranean-sourced waters are around $\sim 15\permil$

(Celle-Jeanton et al., 2001; Vandenschrick et al., 2002; Frot et al., 2007) and may be as high as $20\permil$ in the eastern Mediterranean (Clark and Fritz, 1997; Ayalon et al., 1998).

Changes in seasonality also have a strong control on mean annual $\delta^{18}O$ values, such that the relative proportions of summer vs. winter and their related changes in moisture source may result in abrupt variation in $\delta^{18}O$ values on paleoclimate time scales (Wang et al., 2001; Denton et al., 2005). Because moisture source may vary under different climate regimes (Charles et al., 1994), the strict use of the modern temperature-dependent spatial isotope gradients as a proxy for temporal variations may be problematic. Greenland is a good example, in that changes in the $\delta^{18}O$ value preserved in glacial ice that had been previously interpreted to reflect a temperature change may in fact partly record a change in the moisture source (Charles et al., 1994; Jouzel et al., 1997), which may be tracked with deuterium excess (Dansgaard, 1964; Rozanski et al., 1993; Werner et al., 2001).

The $\delta^{18}O$ value of the ocean has varied on glacial/interglacial time scales via the ice volume effect. Because evaporation of ocean water preferentially removes the light stable isotopes into the vapor, the $\delta^{18}O$ value of the ocean will increase as the volume of freshwater stored on the continents as ice increases. The magnitude of the $\delta^{18}O$ increase is ~ 1.0–$1.2\permil$ during maximum Quaternary ice volume (Schrag et al., 1996, 2002; Lea et al., 2002; Sharp, 2007). The late Quaternary history of ocean water $\delta^{18}O$ variation has been deconvolved from the $\delta^{18}O$ value of marine organisms by subtracting out that component of the variation that is driven by temperature, using Mg/Ca ratios as a proxy (Lea et al., 2002; Fig. 7). The $\delta^{18}O$ of the ocean varies on orbital time scales, thus, the $\delta^{18}O$ values of vapor and the subsequent condensates that contribute to cave recharge may then also vary by up to $1.2\permil$ related to changes in ice volume.

It may be warranted to correct speleothem $\delta^{18}O$ time series by $\delta^{18}O$ changes in the oceanic moisture source (Grootes, 1993), though this practice has not been widely adopted in the international speleothem literature. Changes in $\delta^{18}O$ of the ocean on glacial to interglacial time scales are only one variable that could affect
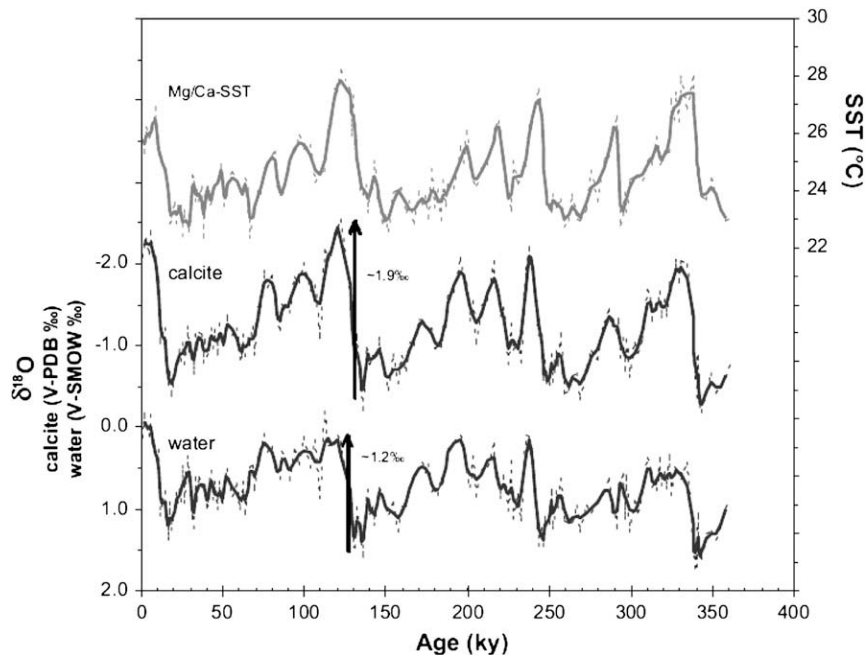
Fig. 7. Variation of the $\delta^{18}O$ value of ocean water (bottom plot) from the tropical Pacific shows orbital-scale changes of up to $1.2\permil$ between glacial and interglacial periods. The variations are forced by changes in continental ice volume, which results in ^{18}O enrichment in ocean waters during maximum ice volume. From Lea et al. (2002). Note that the temporal variation in $\delta^{18}O$ of the ocean is small compared to the spatial variation of $\delta^{18}O$ in precipitation (see Fig. 5).

rainfall $\delta^{18}O$ values. For example, a cooler glacial sea surface temperature and its effect on equilibrium fractionation would result in a rainfall $\delta^{18}O$ decrease to partially or wholly offset the ocean water $\delta^{18}O$ increase. Additional kinetic fractionations may arise from changes in relative humidity and wind speed. As an example, the $\delta^{18}O$ value of the first rain to form from a tropical cloud (from above) is $-2.6\permil$ SMOW. Assuming colder and drier glacial conditions, with $T = 20\,°C$, relative humidity of 75%, and $\delta^{18}O_{ocean} = +1.0$, the $\delta^{18}O$ value of the rain is $-3.5\permil$ SMOW. Thus, the net effect of these presumed glacial boundary conditions is lower $\delta^{18}O_{rain}$ values, despite the higher $\delta^{18}O_{ocean}$, given the assumption that other climatically relevant conditions remain constant. Additional insight into the complex controls on $\delta^{18}O$ values in ice precipitation comes from a modeling study of the $\delta^{18}O$ value of atmospheric vapor and precipitation at the last glacial maximum (LGM) (Lee et al., 2008). These results showed nearly identical $\delta^{18}O_{LGM}$ values to the modern between $20°$ and $45°S$, with lower values by 2–$4\permil$ between ~ 45 and $70°S$.

In reality, combinations of several isotope effects on the mean annual and seasonal $\delta^{18}O$ values are likely for each region (Lawrence et al., 1982; Grootes, 1993; Vimeux et al., 2005; Vuille and Werner, 2005). On continental scales, the strength of the temperature and precipitation amount effects on $\delta^{18}O$ of rain may vary substantially. For example, the southern regions of Asia under the influence of the summer monsoon are dominated by an amount effect, whereas northern areas are dominated by a temperature effect, with an intermediate response in between (Johnson and Ingram, 2004). This result appears valid for other continents between a dividing line at approximately $30°N$ and S latitudes (Vuille et al., 2005; Bowen, 2008).

2.4. Correlations to ocean–atmosphere phenomena

But what climate processes force precipitation $\delta^{18}O$ variability? Interpretation of speleothem $\delta^{18}O$ time series is most useful to climate scientists when correlated to ocean–atmosphere phenomena such as the El Niño/Southern Oscillation (Ropelewski and Halpert, 1987), ITCZ migration (Hastenrath, 2002), North Atlantic Oscillation (Hurrell et al., 2003), or other processes. However, few such speleothem $\delta^{18}O$/ocean–atmosphere process studies have yet attempted such a correlation, because of the difficulty of establishing calibrations between speleothem $\delta^{18}O$ and climate indices over the modern period.

Linear correlation and isotope-labeled modeling studies provide some of the strongest evidence for links between the $\delta^{18}O$ value of precipitation and ocean–atmosphere processes (Jouzel et al., 1997; Cole et al., 1999; Schmidt et al., 2007). For example, the influence of the El Niño/Southern Oscillation on the $\delta^{18}O$ of tropical precipitation has been investigated by both correlation and modeling studies (Vuille and Werner, 2005; Schmidt et al., 2007). Over the tropical Americas, El Niño events are typically associated with below normal rainfall in the northern neotropics. The drier than average conditions results in higher $\delta^{18}O$ values, consistent with the tropical "amount effect". However, in some cases precipitation $\delta^{18}O$ may vary without a change in total precipitation, thus implicating a strong role for regional climate variation in forcing precipitation $\delta^{18}O$ values (Vuille et al., 2005; Schmidt et al., 2007; Sturm et al., 2008). In the Asian monsoon region, an isotope-labeled model simulated the $\delta^{18}O$ values of rainfall with monsoon intensity strength, and was validated by comparison to the GNIP observational network (Vuille et al., 2005). The advantage of modeling is that the $\delta^{18}O$/climate relationship may be calibrated against modern observations and extended to broad areas (IAEA/WMO, 2004). For example, model output suggests that precipitation $\delta^{18}O$ anomalies may be more regionally coherent than the precipitation amount anomalies (Schmidt et al., 2007). Modeling may also

provide estimates of precipitation $\delta^{18}O$ in the past under different orbital boundary conditions (e.g. the mid-Holocene; Schmidt et al., 2007). Significant advances in understanding $\delta^{18}O$/climate relationships can be made with models, and future efforts would benefit from collaborations between speleothem and climate researchers.

3. $\delta^{18}O$ variations in the soil zone and epikarst

3.1. Processes in the soil zone

The $\delta^{18}O$ value of soil water is largely determined by the $\delta^{18}O$ of precipitation of a sufficient intensity to infiltrate soil pores. Infiltration into the soil zone and epikarst is a fraction of mean annual precipitation, as some water must be lost to evaporation, transpiration, canopy interception, or runoff (Fetter, 1994). The $\delta^{18}O$ value of soil water is thus the amount-weighted mean of infiltrating waters and it may be further modified by evaporation (Clark and Fritz, 1997; Tang and Feng, 2001). Evaporation will result in increased $\delta^{18}O$ values of soil moisture (Allison, 1982; Tang and Feng, 2001). The magnitude of $\delta^{18}O$ increase will be related to the relative humidity in the soil pores and the evaporated water volume, and $\delta D/\delta^{18}O$ slopes may reach values as low as 2 (Allison, 1982; Barnes and Allison, 1983; Fontes et al., 1986). The most intense rainstorms that commonly have low $\delta^{18}O$ values are likely to dominate recharge into the soil zone, and would tend to counteract the isotopic enrichment associated with evaporation (Dansgaard, 1964; Rozanski et al., 1993; Gat, 1996; Clark and Fritz, 1997). Regions with arid climates are associated with the greatest evaporative enrichments, and in extreme cases all soil water may be evaporated back to the atmosphere. $\delta^{18}O$/depth profiles typically have a zone of stable values at depth beneath the surface where evaporative effects are minimized (Barnes and Allison, 1983; Liu et al., 1995; Tang and Feng, 2001). An additional modification results from mixing of various infiltrating waters, with soil moisture typically having less $\delta^{18}O$ variability than precipitation (Tang and Feng, 2001). Such mixing in some cases appears to be rapid and takes place near the surface (Cruz et al., 2005b).

Plant transpiration does not fractionate (Longinelli and Edmond, 1983; Gat, 1996), so it is unlikely that there will be a direct role of biotic activity on the $\delta^{18}O$ value of water. However, vegetation density and type will affect soil water evaporation by altering the amount of shade and solar radiation reaching the soil surface, and by microclimate effects such as reduced wind speed, for example in a dense forest vs. an open grassland (Moreira et al., 1997). Natural or human-induced vegetation changes on Quaternary timescales (Bradley, 1999) may have resulted in a soil water $\delta^{18}O$ change prior to infiltration into the epikarst, such that $\delta^{18}O$ values in heavily modified human environments may have an anthropogenic imprint.

3.2. Recharge into the epikarst

After passage of the water through the soil zone it reaches the epikarst. The epikarst is the upper surface of the bedrock characterized by solutional features along joint and bedding planes in the (largely) vadose zone (Klimchouk, 2000; Williams, 2008), where water may be stored and mixed (Yonge et al., 1985; Williams, 2008). Flow through the epikarst (Fig. 1) may occur as diffuse seepage through the primary porosity, through secondary porosity such as fissures and joints, and through conduit flow such as cave streams (Gillieson, 1996; Klimchouk, 2000). Recharge may also follow dolines and other karst subsurface drainage like dry valleys in both diffuse and discrete flow (Jones et al., 2000). The epikarst is characterized by complicated fracturing and joint patterns, in addition to solution channels and other features that are capable of

transmitting water laterally and vertically. Each flow type may be associated with recharge of different origins and varying δ^{18}O values, and the water feeding cave drips is the "downstream" combination of the different water types (Long and Putnam, 2004). If recharge water evaporates in air-filled voids its δ^{18}O value will increase. For example, cave seepage waters in semi-arid regions may have δ^{18}O values that are higher than that of mean annual precipitation (Bar-Matthews et al., 1996, 2003; Carrasco et al., 2006).

The timing and amount of recharge to the epikarst region is an important control on the resulting dripwater δ^{18}O values. In the semi-arid Spring Mountains of southern Nevada, for example, recharge into a carbonate aquifer was sampled at a karst spring, and the δ^{18}O values indicated that $\sim$90% of infiltration represents spring snowmelt (Winograd et al., 1998). In contrast, the δ^{18}O value of cave drip waters appears to be a good reflection of the weighted mean annual δ^{18}O value of precipitation in the eastern United States (Yonge et al., 1985), and the δ^{18}O values of cave drip waters in Kahf Defore cave, southern Oman – in an arid climate – are nearly identical to the δ^{18}O values of rainfall in the area (Fleitmann et al., 2004) indicating only a small amount of evaporation. δ^{18}O values of cave seepage waters from Kentucky (Great Onyx Cave) plot together with precipitation and spring waters on the meteoric water line, suggesting that their values have not been modified substantially by kinetic processes (Harmon, 1979). A study of the δ^{18}O values of wells, springs, and cave drips suggests that the Pleistocene aquifer on Barbados is only recharged by 10–20% of the mean annual precipitation, and that recharge occurred primarily in the wettest periods (Jones et al., 2000) when rainfall exceeded 195 mm/month. This results in the average δ^{18}O value of groundwater (-3.0‰) being lower than the annual weighted δ^{18}O value of rainfall (-1.9‰) (Jones et al., 2000). Maximum infiltration associated with heavy rainfall events may be prevalent, as a study of canopy interception in the humid tropical rainforest of Panama showed that only $\sim$50% of the total rainfall amount transited to the soil zone for potential recharge (Read, 1977), and deep soil water (New Hampshire, USA) only appeared to have been recharged when precipitation was greater than 200 mm (Tang and Feng, 2001).

The transit times of water in the vadose zone may be estimated via lag times of δ^{18}O values in drip waters relative to rainfall amounts (Ayalon et al., 1998; Long and Putnam, 2004; Baldini et al., 2006; Cobb et al., 2007), with chemical variations in karst waters (Even et al., 1986), delay in drip response to rainfall events (Cruz et al., 2005b; Mattey et al., 2008), from fluorescence of drip waters (Baker et al., 1999), and has been estimated with ^{3}H/^{3}He methods (Yamada et al., 2008). The transit time would be most rapid for the conduits, and slowest for the diffuse seepage flow. In a general sense and all other factors being equal, the thicker the overlying limestone the longer the potential transit time and the greater the groundwater mixing. An understanding of drip water transit times is important for the interpretation of speleothem δ^{18}O time series, because systems with a shorter residence time will be more suitable for capturing rapid, high-frequency climate events (McDonald et al., 2007), whereas a very slow transit time with substantial mixing will be more suited for constraining longer-term climate change. A few studies are highlighted here. In tropical Borneo, the δ^{18}O values of rainfall and cave drip waters were determined by measurement over a three-year period (Cobb et al., 2007). Dripwater δ^{18}O values tracked rain δ^{18}O, suggesting a transit time of less than six months consistent with rapid infiltration in a wet tropical environment. Alternatively, measurements of tritium, a radioactive isotope of hydrogen produced by nuclear bomb testing in the 1960s, have shown that transit times in some springs in Turkey were on the order of 20–100 years (Dincer and Payne, 1971), and

that cave drip waters in Soreq Cave, Israel, were several decades old (Even et al., 1986).

The saturation state of drip water may vary over time, thus influencing timing of calcite deposition (Treble et al., 2005b; Baldini et al., 2006). Only those recharge waters that are saturated with CaCO$_3$ will participate in the deposition of speleothem CaCO$_3$. It is this isotopically effective recharge that is relevant to the interpretation of speleothem δ^{18}O time series. The timing of the isotopically effective recharge may be forced by seasonal variations in drip water and cave air pCO$_2$ which influences drip water degassing rates, and could impart a seasonal bias to the speleothem record if certain months produce more calcite than others (Baldini et al., 2008; Mattey et al., 2008). For example, conduit spring waters in Pennsylvania, USA, have been demonstrated to have short residence times and are undersaturated in calcite, whereas diffuse flow springs are saturated with calcite during the winter (Shuster and White, 1972). In this case, if conduit or fracture flow results in rapid transit through the epikarst, the waters may be capable of dissolving calcite within the cave system, particularly if the waters have been charged with CO$_2$ due to biologic respiration in the absence of significant calcite dissolution. Intense rainfall and rapid infiltration may lead to undersaturated and acidic water infiltration (Baldini et al., 2006) that may lead to solutional "drilling" of stalagmite tips (Fig. 8). Ideally, comprehensive studies of infiltration and drip water geochemical measurements (δ^{18}O, pH, pCO$_2$, calcite saturation indices) over the course of several years should be completed to understand the timing of drip and saturation variations (Baldini et al., 2006; Mattey et al., 2008).

Fig. 8. Solutional drilling of a stalagmite tip in Juxtlahuaca Cave, Mexico, by under-saturated drip waters, has created an $\sim$2 cm deep dissolution dish. Such water does not represent isotopically effective recharge. Photo by Matthew Lachniet.

4. $\delta^{18}O$ in the cave system

4.1. $\delta^{18}O$ values of cave drip waters

The $\delta^{18}O$ value of cave drip waters is a function of seasonality of recharge and modification within the soil and epikarst (Fig. 1). Typically, drip water $\delta^{18}O$ variability is attenuated relative to precipitation $\delta^{18}O$ due to mixing in the soil zone and epikarst (Perrin et al., 2003; Cobb et al., 2007; Mattey et al., 2008). The $\delta^{18}O$ value of drip waters may be increased by evaporation in caves with low relative humidity or air circulation. Most caves lacking large openings to the surface are characterized by relative humidity values at or near 100% (Poulson and White, 1969) particularly in humid regions (Lachniet et al., 2004a; Cruz et al., 2005b; Cobb et al., 2007), but also in the sub-humid zone (Bar-Matthews et al., 1996; Frisia et al., 2002). Evaporation would tend to be the greatest when relative humidity is low, the drip has a long residence time on a stalactite or stalagmite tip, and/or the cave is windy and well ventilated. For example, drip waters originating from evaporative "popcorn" calcite deposits in Carlsbad Caverns, New Mexico, USA, have $\delta^{18}O$ values >2‰ higher than other drips (Ingraham et al., 1990). In contrast, little drip water evaporation would be expected in poorly ventilated caves where the relative humidity approaches saturation, particularly for drips with short residence time. In humid (~100% relative humidity) Santana Cave in southeastern Brazil, the $\delta^{18}O$ values of drip waters and the cave pools that they feed are the same, indicating little or no evaporation (Cruz et al., 2005b). In some cases, drip water evaporation may be a paleo-environmental indicator. In tropical regions where the amount effect is dominant, drip water evaporation during periods of reduced rainfall and slower infiltration rates would increase the drip $\delta^{18}O$ value in the same sense as the amount effect (Fleitmann et al., 2004; Lachniet et al., 2004b).

In order to constrain the controls on drip water $\delta^{18}O$, modern observations of drip water geochemistry, cave climate, and atmosphere climate are desirable. For example, a study in Israel (Soreq Cave) demonstrated two drip types, slow drips associated with stalactite tips that represent vadose seepage water that has resided in the aquifer for perhaps a few decades, and fast drips, which originate from intense rainfall events that infiltrate the cave as vadose flow through fractures and fissures, but which also contains a portion of slow-drip waters (Ayalon et al., 1998). Groundwater $\delta^{18}O$ values are nearly the same as the fast-drip waters, indicating that heavy rainfall events are the most likely source contributing to cave waters. Shallow fast drips showed an almost immediate response to heavy rainfall events and the $\delta^{18}O$ values may vary widely, indicating incomplete mixing in the soil and epikarst zones. Heterogeneities of drip rate may also impact paleoclimatic interpretation of $\delta^{18}O$, as the paleoclimatic signal may vary between slow and fast drips (Baldini et al., 2006; McDonald et al., 2007).

4.2. Equilibrium fractionation between water and carbonate phases

In order for speleothems to reliably track changes in the $\delta^{18}O$ values of the cave drip waters, isotopic equilibrium between the water and dissolved and precipitated carbonate phases must be established (Hendy, 1971). Isotopic fractionation occurs at the ambient cave temperature, which is imparted to the cave drip waters due to thermal equilibration between water and rock in the vadose zone (Ayalon et al., 1998; Frisia et al., 2002). Isotopic exchange between the various carbonate phases and the water will result in an equilibrium isotopic value that is dominated by the largest reservoir, in this case the water which contains ~10^4 more oxygen atoms than the carbonate species (Dreybrodt, 2008). Conditions of isotopic equilibrium are likely to be met when sufficient time is available for the isotope exchange reactions to take place (Hendy, 1971; Sharp, 2007).

The temperature-dependent oxygen-isotope equilibrium fractionation between water and precipitated $CaCO_3$ results in the preferential incorporation of ^{18}O in the $CaCO_3$, which has stiffer bonds (Sharp, 2007). The equilibrium fractionation is also dependent upon the carbonate mineralogy, e.g. calcite vs. aragonite (Fig. 9), the latter commonly precipitating from drip water with a high magnesium content (Gonzalez and Lohmann, 1988). An equilibrium fractionation factor relationship was determined for synthetic calcite (Kim and O'Neil, 1997):

$$1000 \ln \alpha_{(calcite-water)} = 18.03\left(10^3 T^{-1}\right) - 32.42 \qquad (10)$$

where $1000 \ln \alpha_{(calcite-water)}$ is the fractionation between the calcite and water, and T is the temperature in Kelvin. $1000\ln \alpha$ values range from 26.12 to 33.62‰, and the slope of the $d\delta^{18}O_{ct}/dT$ in Eq. (10) ranges from -0.18 to -0.23‰ $°C^{-1}$, for temperatures of 35 °C and 5 °C, respectively. A calibration of $\delta^{18}O$ in calcite and water from Devils Hole (Coplen, 2007) suggests a different fractionation that conflicts with previous studies (Kim and O'Neil, 1997), but is at odds with experimental and theoretical results (Chacko and Deines, 2008).

Several studies have derived independent aragonite fractionation factors that may differ from each other significantly (Tarutani et al., 1969; Grossman and Ku, 1986; Zhou and Zheng, 2003; Kim and O'Neil, 2005; Horita and Clayton, 2007; Zheng and Zhou, 2007). The most current fractionation equation for synthetic aragonite (Kim et al., 2007) is

$$1000 \ln \alpha_{(aragonite-water)} = 17.88\left(10^3 T^{-1}\right) - 31.14 \qquad (11)$$
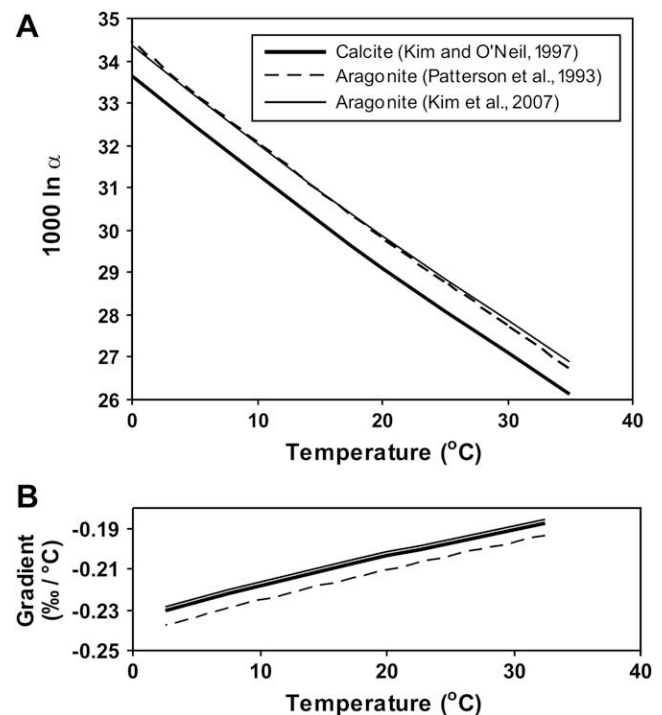
Fig. 9. A) Equilibrium $\delta^{18}O$ fractionation between water and $CaCO_3$ (1000ln α) as a function of temperature. Under equilibrium conditions, aragonite will be precipitated with $\delta^{18}O$ values ~0.7 to 0.8‰ higher than calcite. B) Gradient of $\delta^{18}O$ equilibrium fractionation as a function of temperature, units of ‰/°C; for calcite (Kim and O'Neil, 1997) and aragonite (Patterson et al., 1993; Kim et al., 2007), the gradients vary from -0.18‰/°C at 35 °C to -0.23‰/°C at 5 °C for calcite.

which is virtually identical to the fractionation factor derived for biogenic aragonite from fish otoliths (Patterson et al., 1993):

$$1000 \ln \alpha_{(aragonite-water)} = 18.56 \left(10^3 T^{-1} \right) - 33.49 \qquad (12)$$

Under equilibrium conditions, aragonite should have $\delta^{18}O$ values $\sim 0.8\permil$ higher than calcite at 25 °C (Kim et al., 2007). These equations are consistent with experimental work (Tarutani et al., 1969) and $\delta^{18}O$ measurements indicating ~ 0.6–$1.4\permil$ higher $\delta^{18}O$ values in aragonite than in co-occurring calcite in Carlsbad Caves, New Mexico, USA, (Gonzalez and Lohmann, 1988) and in the Grotte De Clamouse, France (Frisia et al., 2002; McMillan et al., 2005). There is also evidence that the oxygen-isotope fractionation between dissolved inorganic carbon (DIC) and water is pH-dependent (Beck et al., 2005). Calcite deposited from drips at low super saturation, as evident from calcite fabrics, may be the best for representing isotopic equilibrium (Frisia et al., 2000).

To test for equilibrium speleothem calcite precipitation, the $\delta^{18}O$ values of the water and precipitating calcite should be measured along with the drip and cave temperature. The measured $\delta^{18}O$ value of the contemporaneous calcite should equal (within measurement error) the calculated $\delta^{18}O$ value of the speleothem at the cave temperature and measured drip water $\delta^{18}O$ value. For example, calcite rafts and other speleothems in Soreq Cave, Israel were determined to have been precipitated in isotopic equilibrium based on these three measurements (Bar-Matthews et al., 1996), and the $\delta^{18}O$ values of soda straw stalactites coupled with the measured cave temperature in Great Onyx Cave, Kentucky yielded a $\delta^{18}O$ water value that is statistically identical to that measured (Harmon, 1979).

4.3. Kinetic fractionation between water and carbonate

4.3.1. Kinetic fractionation

Kinetic fractionation is associated with incomplete or rapid reactions in which equilibrium between phases is not maintained, such as during fast and/or extensive CO_2 degassing (Hendy, 1971). Such kinetic effects have been suggested to result in oxygen and carbon isotope covariation (Fornaca-Rinaldi et al., 1968; Fantidis and Ehhalt, 1970). The rate of CO_2 degassing is a function of the pCO_2 gradient between the drip, which is largely determined by the degree of biological respiration in the soil zone and the cave atmosphere (Baldini et al., 2008). In well-ventilated cave passages, the pCO_2 is that of the atmosphere, ~ 280 ppm for the pre-Industrial Holocene period. In contrast, pCO_2 values of drip waters may be an order of magnitude larger (Holland et al., 1964). In poorly ventilated caves, pCO_2 values may be very high (Gillieson, 1996), which would limit the pCO_2 gradient between drip and passage. Large pCO_2 gradients between the drip and cave atmosphere favor rapid degassing, which may result in an enrichment in ^{18}O due to isotopic disequilibrium in the precipitated carbonate (Hendy, 1971). For example, extensive drip CO_2 outgassing associated with frost-work aragonite is a likely contributor to high $\delta^{18}O$ values (Frisia et al., 2002).

Some caves clearly precipitate calcite out of equilibrium with drip waters. In Barbados, $\delta^{18}O$ was measured on stalagmite tips and calcite precipitated on flat glass plates placed beneath drips (Mickler et al., 2004, 2006). The cave environment was expected to be favorable for equilibrium fractionation because of high relative humidity and a slow and steady drip rate. However, the $\delta^{18}O$ values of stalagmite tips and glass plate calcite were higher than equilibrium by up to $2.3\permil$, and calcite from the glass plates showed an increase in $\delta^{13}C$ and $\delta^{18}O$ away from the locus of calcite deposition. Mickler et al. (2004, 2006) describe two possible scenarios that may result in ^{18}O enrichment in precipitated calcite. First, if CO_2 degassing was more rapid than CO_2 hydration and hydroxylation,

the $\delta^{18}O$ value of the $HCO_3^-{}_{(aq)}$ may depart from equilibrium with the water (Mickler et al., 2006). The $\delta^{18}O$ of the DIC would increase as ^{18}O-depleted CO_2 is lost to degassing. Thus, the precipitated calcite would have higher $\delta^{18}O$ values than equilibrium as the reaction proceeds due to Rayleigh distillation. Second, if calcite precipitation is rapid then the fractionation between $CaCO_{3(s)}$ and $HCO_3^-{}_{(aq)}$ may be incomplete and approach zero (Michaelis et al., 1985; Mickler et al., 2004). The resulting calcite would theoretically have $\delta^{18}O$ values up to $6\permil$ higher than at equilibrium. This mechanism was also suggested for the rapid precipitation of $CaCO_3$ from a spring in Germany, where no fractionation was observed between $CaCO_{3(s)}$ and $HCO_3^-{}_{(aq)}$ (Michaelis et al., 1985). Kinetic $\delta^{18}O$ fractionation of $\sim +3\permil$ was noted from rapid calcite precipitation from the freezing of natural calcite-saturated waters (Clark and Lauriol, 1992). For laboratory solutions, ^{18}O enrichments averaged $5.5 \pm 0.5\permil$ for the cryogenic calcite (Clark and Lauriol, 1992). In a review of cryogenic calcites, various degrees of oxygen equilibrium and disequilibrium were noted, revealing many complexities of $\delta^{18}O$ in cold-climates (Lacelle, 2007). Only cold-climate speleothems, cryogenic aufeis (ice formed from freezing of spring discharge) forming in zones of limestone bedrock, and biogenic (methanogenic bacteria) calcite precipitates in limestone (endostromatolites) were near oxygen-isotope equilibrium with parent waters (Lacelle, 2007).

4.3.2. The Hendy test

Because kinetic fractionation may obscure or efface the primary climate signal preserved in speleothem calcite, assessment of the degree of isotopic equilibrium is essential for interpreting speleothem $\delta^{18}O$ as paleoclimate records. To evaluate kinetic fractionation in speleothem calcite, it has been recommended to analyze $\delta^{18}O$ and $\delta^{13}C$ both from a single growth layer and along the stalagmite axis with the so-called "Hendy" test (Hendy, 1971). Conditions indicative of kinetic fractionation are 1): an increase in carbonate $\delta^{18}O$ values with distance away from the growth axis; 2) positive covariation between $\delta^{18}O$ and $\delta^{13}C$ along a growth layer; and 3) $\delta^{18}O/\delta^{13}C$ covariation along the growth axis.

Such tests have been widely applied in the literature, but recent results show that some stalagmites might fail a Hendy test yet still represent isotopic equilibrium conditions. For example, experimental and modeling results demonstrate that the first calcite to be precipitated from a solution that undergoes rapid degassing may be deposited in isotopic equilibrium, despite covarying $\delta^{18}O$ and $\delta^{13}C$ away from the growth axis (Dreybrodt, 2008; Wiedner et al., 2008). Such data would fail a Hendy test, yet the $\delta^{18}O$ (and $\delta^{13}C$) values of the stalagmite tip may still represent isotopic equilibrium (Dreybrodt, 2008; Romanov et al., 2008). In support of these modeling studies, Hendy tests on an Austrian stalagmite show stable $\delta^{18}O$ values within 20 mm of the growth axis but high values away from the axis (Spötl and Mangini, 2002).

The application of the Hendy test is also complicated by sampling protocol concerns, and because oxygen and carbon isotopes may covary for climatic reasons. First, it is difficult to accurately subsample calcite of precisely the same age along growth laminae that thin away from the axis (Mickler et al., 2006; Dreybrodt, 2008), a problem that becomes particularly acute when $\delta^{18}O$ varies on small spatial (sub-mm) scales (Treble et al., 2005b). Second, there may be climatic controls on $\delta^{18}O/\delta^{13}C$ covariation, and kinetic fractionation of oxygen isotopes may not necessarily efface the climatic signal (Mickler et al., 2006; Mattey et al., 2008). For example, in the desert southwestern U.S., soil CO_2 $\delta^{13}C$ values decrease with increasing altitude (and decreasing $\delta^{18}O$) (Quade et al., 1989), such that $\delta^{18}O$ and $\delta^{13}C$ covary in pedogenic calcites for climatic reasons. $\delta^{18}O/\delta^{13}C$ covariation may arise in the humid tropics via the amount effect on rainfall and enhanced biogenic respiration during wet periods. Increased rainfall (and by inference

low δ^{18}O values) resulted in low leaf δ^{13}C values in a seasonally dry forest in Costa Rica (Leffler and Enquist, 2002), such that drip waters equilibrated with the decomposing leaves may result in isotope covariation. A similar relationship was noted from a 780-yr long stalagmite record from Oman, where covarying δ^{18}O and δ^{13}C were negatively correlated with annual layer thickness (a proxy for wetness) (Burns et al., 2002; Fleitmann et al., 2004). In some stalagmites from Israel (Bar-Matthews et al., 1999) δ^{18}O and δ^{13}C positively covary yet the δ^{18}O paleoclimate record is tightly correlated with global climate changes.

The studies suggest that stalagmites formed out of isotopic equilibrium may (but not necessarily) preserve paleoclimate information suitable for testing hypotheses of climate forcings and teleconnections, even if the data fail Hendy tests. Although no single test can constrain equilibrium vs. non-equilibrium calcite δ^{18}O in the past, greatest confidence in the climate signal is obtained by replication from multiple stalagmites or by calibration with modern climate records (discussed below). Lack of replication indicates possible kinetic effects. Several studies have replicated speleothem δ^{18}O time series, for example from China (Wang et al., 2001; Cheng et al., 2006), and the mid-continental US (Dorale et al., 1998; Denniston et al., 1999). The presence of the same, or highly similar, δ^{18}O record across several time-overlapping stalagmites, rooted to a firm chronology, is probably the best evidence of a high fidelity paleoclimatic signal in stalagmites (Wang et al., 2001).

5. Paleoclimatic interpretation of speleothem δ^{18}O time series

5.1. Quantitative paleotemperature estimates

Interpretations of speleothem δ^{18}O time series have been both quantitative and qualitative. Although speleothems showed considerable initial promise as continental paleotemperature archives, few reliable estimates have been published because of the considerable complexity of δ^{18}O in the atmosphere, hydrosphere, and cave environment. In particular, knowledge of the MAT of the site, cave temperature, and δ^{18}O value of the drip water are required to estimate quantitatively past temperatures from speleothem δ^{18}O data. The classic paleotemperature equation (Epstein et al., 1953), which may also be used to assess isotopic equilibrium, can be defined in terms of both the PDB and SMOW scales (Sharp, 2007):

$$T\ (^{\circ}C) = 15.75 - 4.3(\delta^{18}O_{calcite-PDB} - \delta^{18}O_{water-SMOW})$$
$$+ 0.14(\delta^{18}O_{calcite-PDB} - \delta^{18}O_{water-SMOW})^2 \quad (13)$$

where PDB and SMOW refer to the values on their respective scales. As the equation contains two unknowns (T and $\delta^{18}O_{water}$) and only one measured value ($\delta^{18}O_{calcite}$), independent estimates are required of either T or $\delta^{18}O_{water}$ for times in the past.

Two sources to estimate the $\delta^{18}O_{water}$ have been identified: 1) groundwater of known age and isotopic composition from near the studied cave, and 2) fluid inclusions within speleothem calcite. For example, a stalagmite from South Africa (Talma and Vogel, 1992) dated by ^{14}C and U-series methods (Holmgren et al., 1995) was used to estimate late Quaternary paleotemperatures. The δ^{18}O value and ^{14}C age of artesian aquifer water 350 km east of the cave were also determined. Substitution of measured δ^{18}O values of the stalagmite carbonate and inferred drip water from the aquifer water analysis into the paleotemperature equation indicated temperatures 5–7 °C lower during the late glacial relative to modern.

The estimation of dripwater δ^{18}O from the δD value of fluid inclusions (Matthews et al., 2000; Dennis et al., 2001) may also allow estimation of paleotemperatures. Because the δ^{18}O value of entrapped inclusion water may have undergone isotopic exchange

with the surrounding calcite, the inclusion δD value is used to calculate the original inclusion water δ^{18}O value using the local or global meteoric water line, with the estimated value substituted in the paleotemperature or fractionation equations. Although technique-dependent fractionation of δD values may be up to $-30‰$ relative to entrapped drip water (Matthews et al., 2000), technical advances may help to reduce or eliminate the fractionation. Fluid inclusion extractions have precisions of 3‰ δD and 0.4‰ δ^{18}O (Dennis et al., 2001). In rare cases, macroscopic fluid inclusions are present in stalagmites, which allow direct measurement of δ values (Genty et al., 2002).

A key assumption in using fluid inclusion δD to infer the drip water δ^{18}O value is that the slope of the past meteoric water line is known. Use of an incorrect meteoric water line may result in significant errors in the paleotemperatures. For example, assuming a measured fluid inclusion δD value of $-40‰$ SMOW, a measured stalagmite δ^{18}O value of $-8.26‰$ PDB, and the global meteoric water line of $\delta D = 8 \times \delta^{18}O + 10$ results in a calculated δ^{18}O value of the dripwater of $-6.25‰$ and a paleotemperature of 24.96 °C. Using a more evaporative MWL of $\delta D = 5 \times \delta^{18}O - 15$, the calculated δ^{18}O value of the drip water is $-7.00‰$ SMOW, and the calculated paleotemperature is 21.39 °C. The difference in estimated paleotemperature is 3.57 °C, which is large relative to the range of glacial to interglacial temperature variations in many regions. Thus, independent data constraining the past MWL are useful for the use of δD of fluid inclusions to infer paleotemperature. Alternatively, paleotemperature information from paleoclimate or historical data (Matthews et al., 2000; Frisia et al., 2005), or noble gases in fluid inclusions (Kluge et al., 2008) (a technique that has achieved success in estimating paleotemperature from groundwater (Stute et al., 1992)) may allow determination of the δ^{18}O of past drip water with better confidence.

A recent methodological advance in calculating paleotemperatures from carbonate minerals is "carbonate clumped isotope thermometry" (Ghosh et al., 2006a; Eiler, 2007). The basis of the technique is that the various carbonate multiply substituted isotopologues ("clumps") have temperature-dependent equilibrium constants. The technique measures the concentrations of the clumps, and the relative deviation of their concentrations from a stochastic distribution (Δ) is a function of temperature. The key revolution with this method is that the δ^{18}O value of the precipitating fluid is not required to estimate paleotemperature. Analytical uncertainties limit the precision to ± 2.0 to 4.0 °C (Ghosh et al., 2006b), although at the highest measurement precision the temperature precision may be ± 1.0 °C (Eiler, 2007). The technique has shown merit in the estimation of tectonic uplift via analysis of pedogenic carbonates (Ghosh et al., 2006b), and for the independent estimation of Phanerozoic paleotemperature (Came et al., 2007). The technique will need additional improvement in availability and analytical precision in order to be applied to precise determination of late Quaternary paleoclimate questions associated with speleothems.

5.2. Semi-empirical δ^{18}O/climate relationships

An alternative approach to paleotemperature estimation is based on the combined relationship between temperature and the δ^{18}O value of rainfall and the effect of cave temperature on the equilibrium fractionation associated with calcite precipitation. The first control is the mean annual temperature (MAT) of the site and its relationship to the δ^{18}O value of precipitation ($d\delta^{18}O_p/dT$). This expression is related to the well-known positive correlation between rainfall δ^{18}O and MAT that is valid for mid- to high-latitude regions (Dansgaard, 1964; Rozanski et al., 1993). The second temperature control is the cave temperature and its effect on the temperature-dependent fractionation of oxygen isotopes during

calcite precipitation ($d\delta^{18}O_{ct}/dT$), where there is an inverse relationship between cave temperature and calcite $\delta^{18}O$ (Duplessy et al., 1970; Schwarz, 1986; Gascoyne, 1992) as a function of the temperature-dependent fractionations discussed above (Kim and O'Neil, 1997; Kim et al., 2007). For temperatures between 5 °C and 30 °C, the slope of this relationship is -0.18 to $-0.23\permil \cdot °C^{-1}$ (Fig. 9). For a glacial temperature reduction of 5 °C and assuming dripwater $\delta^{18}O$ remained constant, glacial age calcite would be higher by $\sim 1\permil$.

Because both $d\delta^{18}O_p/dT$ and $d\delta^{18}O_{ct}/dT$ affect the speleothem $\delta^{18}O$ value, they can be combined to estimate a single $d\delta^{18}O/dT$ relationship for a studied cave (Gascoyne, 1992; Williams et al., 1999). For example, a $d\delta^{18}O_p/dT = +0.6\permil$ was combined with $d\delta^{18}O_{ct}/dT = -0.26\permil \cdot °C^{-1}$ temperature-dependent fractionation to result in an $\sim +0.34\permil \cdot °C^{-1}$ relationship of speleothem calcite to MAT (Dorale et al., 1998). Another example was used for a stalagmite collected from the Austrian Alps (Mangini et al., 2005), which determined a transfer function from combining the temperature-dependent fractionation of calcite of $-0.22\permil \cdot °C^{-1}$, and an estimate of the $d\delta^{18}O_p/dT$ for periods with independent constraints $-0.44\permil \cdot °C^{-1}$ to yield an overall temperature effect of $-0.22\permil \cdot °C^{-1}$. The two cases reveal an opposite response of calcite $\delta^{18}O$ to temperature: positive in the first case, and negative in the second case, which suggests that local conditions must be known in order to estimate paleotemperatures (semi-)quantitatively. The above approach is complicated by considerable evidence that suggests $d\delta^{18}O_p/dT$ has changed significantly over time (see Section 2.3), and considerable error may be introduced into a paleotemperature estimate if the incorrect slope is chosen.

Because tropical rainfall is dominated by the amount effect ($d\delta^{18}O_p/dP$), it should be theoretically possible to quantify past rainfall from the $\delta^{18}O$ values of speleothem calcite if the $d\delta^{18}O_p/dP$ relationship is known. However, only a few quantitative applications of a $\delta^{18}O_p/dP$ relationship to speleothem $\delta^{18}O$ variations have been published (Bar-Matthews et al., 2003; van Breukelen et al., 2008). Based on a $d\delta^{18}O_p/dP$ gradient of $-1.02\permil/200$ mm for annual rainfall in Israel, paleorainfall estimates for speleothem calcite were estimated for interglacial periods when the slope of the gradient was most likely to have been the same as today (Bar-Matthews et al., 2003). However, such calibrations have been rarely exploited for the primary reason that the $d\delta^{18}O_p/dP$ relationship may not have been constant over time. The $d\delta^{18}O_p/dP$ in modern climate is typically based on monthly averages, because long-term annual records of $\delta^{18}O$ in rainfall are lacking from most locations. However, it is not clear how seasonal $\delta^{18}O$ variability can be extrapolated to decadal to millennial-scale stalagmite $\delta^{18}O$ variability, because the seasonal cycle may not be a direct analog for $\delta^{18}O$ variation on longer time scales. Further, the smoothing effect in an aquifer due to mixing of infiltrated waters of varying ages would produce a dampened $\delta^{18}O$ signal in a speleothem, and would underestimate true rainfall variation.

5.3. Speleothem $\delta^{18}O$-climate calibration

Correlations with modern climate data have additional power to reveal $\delta^{18}O$-climate relationships (Burns et al., 2002; Fleitmann et al., 2004; Fischer and Treble, 2008; Mattey et al., 2008). Dendroclimatologists have long completed such calibration studies (Bradley, 1999), which is aided by the robust annual ring chronologies. Such a calibration is rendered more difficult because only some stalagmites contain annual banding (Baker et al., 2008), and uranium-series dating is not suited for sub-decadal resolution of young $CaCO_3$ with typical uranium concentrations of ~ 1 ppm. Physical or geochemical indicators of annual layers may be present in some speleothems, and include annual variations in trace element concentrations (Roberts et al., 1998; Fairchild et al., 2001; Finch et al., 2001), in $\delta^{13}C$ and $\delta^{18}O$ (Treble et al., 2005b; Mattey

et al., 2008), annual petrographic bands (Railsback et al., 1994; Genty and Quinif, 1996; Polyak and Asmerom, 2001), or luminescence banding (Baker et al., 1993; Shopov et al., 1994). Other radiogenic isotopes such as ^{210}Pb, ^{137}Cs, and bomb-^{14}C hold considerable promise as chronometers over the past several decades (Genty et al., 1998; Frappier et al., 2002; Mattey et al., 2008).

A case example of modern calibration of stalagmite $\delta^{18}O$ values is from a 780-yr stalagmite from Oman (Burns et al., 2002). Two U–Th ages and annual growth layer thickness measurements (average of 0.35 mm/yr) give this stalagmite a suitable chronology to evaluate the direct $\delta^{18}O$-climate link to gridded annual precipitation anomalies in the Indian Ocean region. The analysis shows a strong visual correlation, such that a change in $\delta^{18}O$ of $0.6\permil$ is associated with a precipitation anomaly of ~ 75 mm ($1\permil/125$ mm). The results demonstrate that the amount effect is the dominant control on stalagmite $\delta^{18}O$ values. Because $\delta^{18}O$ is correlated with annual layer thickness ($r = -0.40$), itself correlated to rainfall amount and growth rate, the stalagmite $\delta^{18}O$ can be considered a proxy for past rainfall amount. It is interesting to note that although the calcite $\delta^{18}O$ values are slightly higher than expected for equilibrium calcite likely due to kinetic fractionation, the stalagmites still reveal a robust correlation to modern climate (Fleitmann et al., 2004). Another example is from the Italian Alps (Frisia et al., 2005). They determined the stalagmite chronology using U-series data and extrapolation of an estimated growth rate of 0.11 μm per year. They compared the stalagmite $\delta^{18}O$ with a reconstruction of alpine temperature anomalies, which shows that a 1 °C rise in mean annual temperature is associated with a $2.85\permil$ increase in stalagmite $\delta^{18}O$ ($r^2 = 0.38$; $r = -0.61$). Further, a high resolution ($\sim$ bi-monthly) 53-yr long isotope record from a stalagmite from Gibraltar shows annual $\delta^{13}C$ cycles, which were used to assign ages to the $\delta^{18}O$ time series with additional anchor points derived from bomb-^{14}C dating and annually resolved trace element concentrations (Mattey et al., 2008). A winter dripwater isotopic reconstruction was derived by conversion of stalagmite $\delta^{18}O$ to drip water $\delta^{18}O$ assuming a constant temperature, and was compared to weighted winter precipitation $\delta^{18}O$. The correlation between the two sets is moderately strong ($r^2 = 0.47$, increasing to $r^2 = 0.57$ if one outlier is removed), and includes an increase in $\delta^{18}O$ over the past three decades that mirrors rising winter temperatures. In addition to an apparent relationship between low $\delta^{18}O$ and wet years, the correlation also suggests a winter temperature control on stalagmite calcite.

6. Sampling protocol and data considerations

The $\delta^{18}O$ sampling protocol for speleothem research has been thoroughly reviewed with examples in (Fairchild et al., 2006; Spötl and Mattey, 2006), but merits some additional consideration. Advances in mass spectrometry, in particular automated and rapid mass spectrometric determination of $\delta^{18}O$ and $\delta^{13}C$ in carbonates, have expanded scientists' ability to reconstruct past climates at very high resolution. Financial considerations notwithstanding, it is a good idea to subsample the speleothem at a resolution an order of magnitude finer than the climate process of interest. To achieve this resolution, three sampling protocol factors should be considered: 1) the diameter of the drill bit and its effect on time averaging for each powdered subsample. Drill bits 1.0 mm or smaller in diameter are suggested. 2) the sampling interval (resolution), e.g. the distance between subsamples. The fidelity of the subsampling to represent the paleoclimate signal will increase up to a point as the sampling resolution increases; and 3) the nature of subsampling, either discreet microdrilling (spot sampling) which may or may not overlap with subsequent subsamples (depending on drill bit size), or micromilling of swaths which removes contiguous sections of

the stalagmite (also referred to as "continuous routing" (Quinn et al., 1996)). In the latter case, milling is likely to have the highest fidelity for the climate signal because of its continuous nature, but requires that swaths of material (typically ∼2 mm wide) parallel to growth banding are removed to generate sufficient $CaCO_3$ for isotopic analysis. The current lower mass limit is ∼10–20 μm for dual inlet stable isotopic analysis (Dettman and Lohmann, 1995; Klein and Lohmann, 1995; Wurster et al., 1999). Micromilling may be impractical in fast-growing speleothems where the temporal resolution between swaths is much smaller than the time scale of interest. One implication of a regular sampling interval is that the subsampled material will be biased toward the time interval associated with the highest growth rate, for example summer vs. winter (Quinn et al., 1996; Baldini et al., 2008).

Development of computer-controlled micromilling provides high resolution, technical simplicity, and continuous sampling (Dettman and Lohmann, 1995; Wurster et al., 1999) with precisions better than 20 μm. A major advantage of computer-controlled micromilling is the ability to digitize complicated sampling and intermediate paths along individual growth laminae, either from images (Dettman and Lohmann, 1995), or directly from the sample mounted on a movable stage in reflected light (Wurster et al., 1999). Micromilling is superior to microdrilling because it does not leave material between samples, and allows increased resolution at a scale finer than the drill bit diameter. A nice test of the effects of micromilling, microdrilling, and laser ablation interfaced to a stable isotope mass spectrometer was performed (Spötl and Mattey, 2006). The results show that high resolution micromilling of 100–250 μm of their stalagmite provided ideal sample resolution. The micromilling captured greater isotopic variability than microdrilling, and is thus likely to better represent true speleothem $\delta^{18}O$ variability (Spötl and Mattey, 2006).

Because aragonite is metastable, conversion to calcite under high temperatures or shear stress during micromilling is possible, although such effects are mostly unconstrained by experimental data. The effect of micromilling on the $\delta^{18}O$ values of biogenic aragonite (Foster et al., 2008) resulted in only minor conversion to calcite (estimated as less than 6%) which had a negligible effect on the $\delta^{18}O$ values. Because many speleothems contain aragonite, careful sampling would avoid overly heating or shearing the sample.

Sampling with laser ablation systems coupled to mass spectrometers has attained a resolution of 250 μm or higher, although the technique may suffer from isotopic fractionation associated with surface irregularities which may produce $\delta^{18}O$ artefacts (Fairchild et al., 2006; Spötl and Mattey, 2006). A comparison of laser ablation and micromilling sampling protocols indicates a high degree of correspondence at ∼300 μm scales, but that the micromilling does not have the associated problems of isotopic fractionation (Spötl and Mattey, 2006). Additional improvements in sampling resolution are obtainable with ion microprobe analysis which may be as precise as 20 μm spacing spot size, but the trade-off is decreased precision and problems with isotopic heterogeneity of standard materials at this fine scale (Kolodny et al., 2003; Treble et al., 2007).

The importance of resolution is evident in the large $\delta^{18}O$ variability on small spatial scales (<1 mm) in many speleothems (Treble et al., 2007). A loss of $\delta^{18}O$ variability in corals of both discreet drill spots and milling was apparent when sampling resolution decreased (Quinn et al., 1996). This effect may also be seen in speleothem carbonate. As an example, 168 carbonate subsamples were micromilled at 100 μm intervals from a Panamanian stalagmite (PN-1), and compared with 1-mm resolution micro-drilled discrete samples using a 0.6-mm-diameter drill bit. Although most of the 100 μm $\delta^{18}O$ variation was less than 1‰, 4.7% of the analyses varied by >1.0‰, and the maximum shift in $\delta^{18}O$

was 3.1‰ (Fig. 10). Such variation was mostly missed by the 1-mm subsampling, which shows the same basic trend but misses some prominent isotopic events. Similar results were noted in a comparison of microdrilling and micromilling (Spötl et al., 2006), and micromilling in comparison to an ion microprobe (Treble et al., 2007).

The problems of aliasing in the subsampling of time series should be considered when adopting a subsampling protocol. Aliasing is the undersampling of a periodic signal that may yield false trends, and may result in an underestimation of the true climate signal variability (Mattey et al., 2008). The problem of aliasing a seasonal cycle in speleothems may be reduced or eliminated by subsampling with a drill bit larger than the annual growth rate or by consecutive micromilling. A statistical test to evaluate for undersampling is to calculate the lagged autocorrelation coefficients (Brockwell, 2002) (ACC; correlate the time series to itself, shifted by one or more data points). A time series with random variability would have an autocorrelation coefficient of $r \approx 0$, whereas r would approach 1.0 in a persistent time series. If the $\delta^{18}O$ time series exhibits a low autocorrelation at small lags, then it means either 1) the climate signal preserved in the stalagmite is inherently noisy, or 2) the speleothem may be undersampled, and much of the true climatic variation has not been captured by the sampling protocol. Increased sampling resolution may help resolve the latter problem. As an example, the lag-1 autocorrelation coefficient for 100 μm-resolution $\delta^{18}O$ data from stalagmite PN-1 is $r = 0.72$, indicating moderately strong autocorrelation. The entire 641-mm-tall stalagmite was also subsampled via microdrilling (0.6 mm-diameter bit) at 1 mm intervals from 9 to 161 mm depth, and at 2 mm intervals from 161 to 641 mm depth. The depth series was statistically interpolated at increasing intervals (1–5 mm) to emulate decreasing sampling resolution. The lag-1 ACCs for the 1, 2, 3, 4, and 5 mm statistically subsampled depth series show a general decrease of $r = 0.79$, $r = 0.45$, $r = 0.54$, $r = 0.34$, and $r = 0.32$, respectively (Fig. 11). Also apparent is the loss of climatic information with decreasing time resolution. In contrast, if a time series exhibits maximum autocorrelation at a particular subsampling interval then a higher resolution would not result in increased signal fidelity and the material and is over sampled (Quinn et al., 1996). For comparison to a very well sampled time series, the lag-1 autocorrelation coefficient calculated for the Greenland Ice Sheet
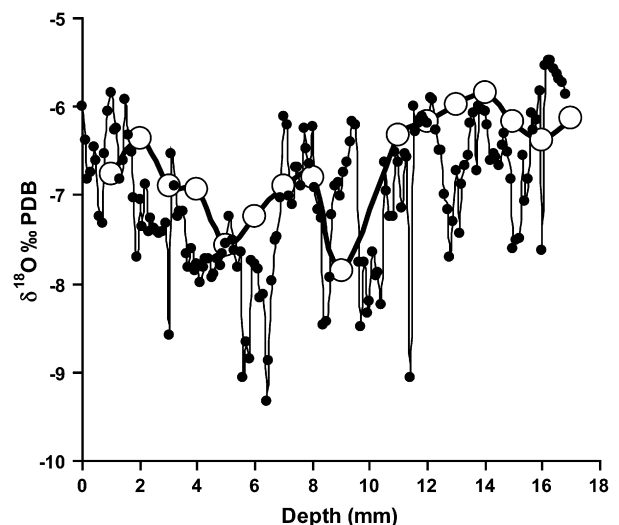

Fig. 10. High resolution (100 μm) subsampling via micromilling of consecutive swaths of calcite from stalagmite PN-1 (black circles) shows substantial point-to-point variability. The low resolution 1-mm spot sampling (white circles) shows that much of the climate signal is lost at the lower resolution.
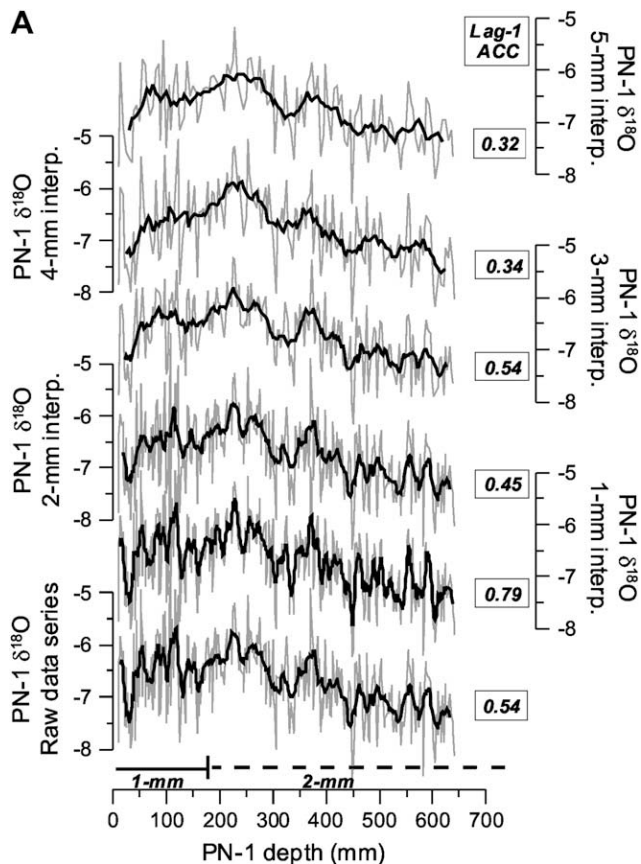
A

Fig. 11. A) Statistical subsampling and autocorrelation coefficients of the stalagmite PN-1 $\delta^{18}O$ depth series. Starting from bottom is the original $\delta^{18}O$ series, followed by 1, 2, 3, 4, and 5 mm linearly interpolated depth series. The bars above the depth axis indicate the drill-subsampling intervals for the raw data series, and the numbers in boxes are the Lag-1 autocorrelation coefficients. The 1-mm interpolation has a higher autocorrelation than the raw data because of the statistical oversampling of the lower resolution (2-mm) raw data drill subsamples. The series are fit with a 9-pt running average (bold line). It is clear that there is a loss of climate signal with the lower subsampling resolution, although the broad trends are maintained. Younger ages are to the left.

drill core (GRIP) (Johnsen et al., 2001) is $r = 0.96$. In this case it is clear that the Panama stalagmite record is either inherently noisier or undersampled relative to the Greenland record.

7. Spatial variations in stalagmite $\delta^{18}O$

To date, little work has explored the spatial variations in isotopic "effects" as preserved in speleothem $\delta^{18}O$ values, such as the altitude, continentality (latitude/longitude), and rainout effects. As speleothem records are become more ubiquitous, such attempts are now feasible. Speleothems should record an altitude effect in their mean $\delta^{18}O$ composition of samples collected within a region. For example, an altitude effect of $\sim -2‰ \, km^{-1}$ in soda straw stalactite $\delta^{18}O$ was noted from New Zealand (Williams et al., 1999), from stalagmites from China (Kong et al., 2005), and in the European Alps (McDermott et al., 1999). $\delta^{18}O$ values of a late Holocene stalagmite from New Zealand demonstrated a latitude effect of $0.33‰/°$ of latitude (Williams et al., 1999), compared to the modern gradient of $0.27‰$ for the $\delta^{18}O$ of precipitation. In southern Brazil, a $\delta^{18}O$ latitudinal gradient of $0.81‰/°$ can be calculated from stalagmites Bt2 and St8 collected from two caves near the Atlantic coast (Cruz et al., 2006). A strong continental effect was observed in $\delta^{18}O$ values of several stalagmites collected across the Central American Isthmus (Lachniet et al., 2007), showing decreasing $\delta^{18}O$

with distance away from the main moisture source of the Caribbean Sea. Further work exploring changing isotope gradients over time has the potential to constrain climate dynamics such as changing moisture source variations over space and time, and allows delineation of shifting climate zones on a global basis. The development of such networks should become a priority of speleothem-based paleoclimate research.

8. Speleothem paleoclimate reveals global teleconnections

Despite uncertainties in $\delta^{18}O$/climate calibrations, speleothem $\delta^{18}O$ time series have permitted unprecedented insight into terrestrial paleoclimates and their links to oceanic and atmospheric climate dynamics. In particular, speleothems have demonstrated a powerful ability to develop a spatial sense of paleoclimatic change by correlation and qualitative visual matching of speleothem $\delta^{18}O$ time series with those derived from marine and ice core records. Though the time series are not interpreted quantitatively, they demonstrate teleconnections between widely separated regions that allow paleoclimatologists to infer climate dynamics. This new approach to speleothem paleoclimatology emphasizes the climate linkages between regions, and the internal and external forcing mechanisms, such as Milankovitch variations (Bradley, 1999), thermohaline circulation variations (Shackleton et al., 2004), and latitudinal displacements of the climatic zones (ITCZ, westerlies, etc.). A few selected case studies (Fig. 12) illustrate these points nicely, and highlight some of the major advances (and controversies) regarding late Quaternary paleoclimate.

The most iconic long-term speleothem $\delta^{18}O$ time series comes from subaqeous vein-filling calcite at Devils Hole, a tectonic fracture in the Basin and Range region of southern Nevada (Winograd et al., 1992). The calcite was dated by U-series methods and $\delta^{18}O$ values revealed significant variation over the past 500 ka. Surprisingly however, the timing of the glacial to interglacial cycles differed significantly from that predicted by Milankovitch solar insolation variations, and of $\delta^{18}O$ variations in marine sediment cores that were chronologically tuned to orbital variations (Winograd et al., 1992). In particular, the timing of most of the glacial to interglacial terminations occurred at times either preceding or not associated with peaks in northern hemisphere summer insolation. Later work indicated that the Devils Hole $\delta^{18}O$ record includes spectral power at bands similar to Milankovitch forcing, and primarily records sea surface temperatures of the California Current (Winograd et al., 2006). Other speleothem and ice core records indicate a later timing of the penultimate glacial to interglacial transition that is consistent with Milankovitch forcing, e.g. in Antarctica, Israel, China, and the Italian Alps (Drysdale et al., 2005). Although the scientific debate on the significance and forcing of the Devils Hole record continues (Herbert et al., 2001, 2002; Winograd, 2002; Yang et al., 2005), the time series does capture long-term and well-dated paleoclimatic variations.

Speleothems have also helped to reveal the spatial fingerprint of rapid millennial-scale climate oscillations during the deglacial and last glacial periods as noted in polar ice cores and North Atlantic marine sediment cores (Stuiver and Grootes, 2000; Johnsen et al., 2001; Augustin et al., 2004; Shackleton et al., 2004), such as rapid warming associated with the Bølling-Allerød (B-A), cooling associated with the Younger Dryas (YD), millennial variability associated with Dansgaard/Oeschger (D/O) events (Johnsen et al., 1992; Dansgaard et al., 1993), and iceberg discharges known as Heinrich Events (Hemming, 2004). Speleothem evidence suggests that the last glacial millennial-scale climate oscillations had a large spatial fingerprint for much of the northern hemisphere. For example, stalagmites from the Asian monsoon region from Hulu Cave, China, were the first to conclusively demonstrate the presence of a millennial-scale monsoon response associated with D/O events
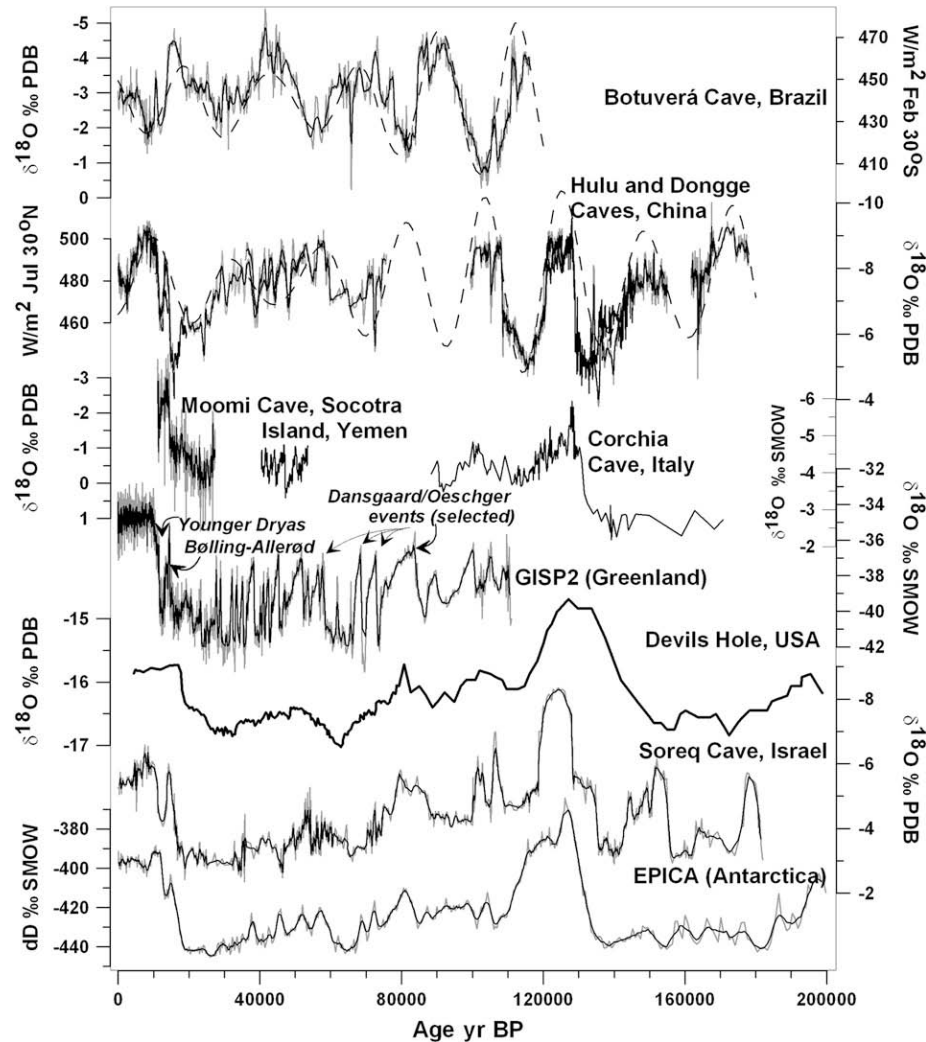
Fig. 12. Selected paleoclimate records from speleothems and ice cores show global climate teleconnections. Speleothem records from the northern hemisphere (e.g. Moomi Cave, Hulu and Dongge Caves, Devils Hole, and Soreq Cave) have a strong imprint of high-latitude climates (Greenland and Antarctica), whereas low-latitude records also contain an imprint of precessional variations (dashed thin lines), e.g. in Brazil (Botuverá Cave), and China (Hulu and Dongge Caves). These climate records demonstrate a robust response of atmospheric circulation to ocean–atmosphere–cryosphere reorganizations. For all records, up is warm and/or wet. There is a clear antiphasing between northern and southern hemisphere monsoon records (Brazil and China) that reflects hemispherically anti-symmetric precessional-scale insolation variations. The raw data series are shown by thin grey lines with a 5-pt running average (thick black line), except for the Devils Hole record, which is the raw data, and the older Moomi Cave record which is a running average. See text for references.

(Fig. 12) via a climate teleconnection to the North Atlantic (Wang et al., 2001), which may be related to a winter season signal related to similar changes in Greenland (Denton et al., 2005). Their replicated stalagmite record, anchored by high-precision U-series dating, shows millennial-scale climate events in the Asian monsoon region which are convincingly correlated to the D/O and Heinrich events from the North Atlantic. Warm periods in Greenland are associated with lower stalagmite $\delta^{18}O$ values, which in this monsoon climate relates to both the amount effect and the seasonal variations of winter vs. summer rainfall. During cool periods apparently coincident with Heinrich events, high $\delta^{18}O$ values may indicate a greater contribution of winter rainfall and are associated with wet periods in the southern hemisphere neo-tropics (Wang et al., 2004), an idea that has support from modeling studies (Chiang et al., 2003). Additionally, the Asian monsoon appeared to vary in strength coincident with the deglacial warming and cooling associated with the B-A and YD events at Hulu and Dongge caves (Wang et al., 2001; Dykoski et al., 2005). Further, the Asian monsoon record has been extended to cover the penultimate glacial and deglacial period (Fig. 12) to reveal additional millennial-scale and insolation control of Asian Monsoon variability (Yuan

et al., 2004; Cheng et al., 2006; Kelly et al., 2006). Decreases in monsoon rainfall have also been linked to the draining of glacial Lake Agassiz in North America at 8.2 ka (Fleitmann et al., 2003; Lachniet et al., 2004a; Dykoski et al., 2005), likely associated with changes in ocean thermohaline circulation.

The impact of apparent D/O events and the Bølling-Allerød on monsoon rainfall is also evident in the $\delta^{18}O$ values of stalagmites collected from Socotra Island, Yemen (Burns et al., 2003; Shakun et al., 2007), in the European Alps (Spötl and Mangini, 2002; Spötl et al., 2006), and in the southwestern United States (Wagner et al., 2005). Socotra Island receives its sparse rainfall from the northern fringe of the ITCZ, so that the rainfall $\delta^{18}O$ values should indicate the intensity of rainfall over the island via the amount effect. Periods of lower $\delta^{18}O$ values (tied to an updated chronology of Burns et al., 2003) are interpreted to reflect enhanced precipitation in the ITCZ, and are convincingly correlated to warm periods in the North Atlantic as evident from Greenland Ice cores (Fig. 12). These data reveal the warm/wet and cold/dry teleconnection between the North Atlantic Ocean and the Indian monsoon, suggesting that monsoon strength in both the Asian and Indian monsoon regions are linked via teleconnections to North Atlantic climate. Additional

evidence for climate teleconnections between the North Atlantic and remote locations comes from $\delta^{18}O$ time series (Fig. 12) from stalagmites from Israel (Frumkin et al., 1999; Bar-Matthews et al., 2003). Increases in stalagmite $\delta^{18}O$ values, were interpreted to reflect cooling forced by Heinrich events and during the last glacial maximum (Bar-Matthews et al., 1999), although some of the Heinrich events in the North Atlantic do not appear to have $\delta^{18}O$ events in the Soreq Cave speleothems. The timing of low $\delta^{18}O$ values coincided with regional wet periods over the past 180 ka during which the distinctive organic-rich sapropels were deposited in the Mediterranean Sea (Bar-Matthews et al., 2000; Ayalon et al., 2002; Bar-Matthews et al., 2003).

Speleothems have also provided evidence that monsoon and climate dynamics in low-latitude regions are partly controlled by solar insolation on precessional time scales. In addition to the above mentioned data, records from the Indian Ocean and South American monsoon regions support the connection between greater summer insolation and a stronger monsoon (Fig. 12). In southern Oman, the intensity of the monsoon appears to be strongly linked to summer insolation over the Holocene period (Fleitmann et al., 2003), as do changes in the strength of the Asian Monsoon (Dykoski et al., 2005). Decreased monsoon rainfall is linked to less northern hemisphere summer insolation, punctuated by centennial- to millennial-scale fluctuations coincident with temperature fluctuations inferred from Greenland Ice cores. In southern South America, subtropical stalagmites show a pronounced Holocene increase in monsoon intensity (Cruz et al., 2005a; Wang et al., 2006; van Breukelen et al., 2008) that coincided with an increase in southern hemisphere summer insolation. In southern Brazil, the stalagmite $\delta^{18}O$ records from Botuverá Cave were interpreted as shifts in the moisture source region and the amount of rainfall, which is driven by circulation patterns that integrate rainout processes upwind of the study area (Sturm et al., 2008). The Brazil records show a strong inverse correlation to Asian Monsoon intensity (Fig. 12), which was interpreted to reflect an interhemispheric antiphasing of tropical rainfall attributed to variations in the north-south position of the ITCZ and areas of greatest monsoon strength (Wang et al., 2006). The strength of the Indian monsoon also appears to be linked to variations in solar variability during the early Holocene (9.6–6.1 ka), as shown by a rainfall periodicity and a strong positive correlation ($r = 0.60$) and phase coherence between stalagmite $\delta^{18}O$ and tree-ring derived $\Delta^{14}C$ (Neff et al., 2001). In the southwestern United States, a region under the influence of the North American Monsoon, $\delta^{18}O$ is negatively correlated ($r = -0.38$) to solar radiation ($\Delta^{14}C$), opposite in sense to data from the Asian and Indian monsoon regions (Asmerom et al., 2007). The opposite 'sense' of the speleothem $\delta^{18}O/\Delta^{14}C$ records was suggested to be related to variations in the Walker circulation associated with the El Niño/ Southern Oscillation, which has opposite effects on the Asian and southwestern U.S. in the modern climate (Asmerom et al., 2007).

9. Summary

Significant advances in the understanding of $\delta^{18}O$ variation in the Earth system have propelled cave speleothems to the forefront of paleoclimatology. In particular, the controls on the fractionation of oxygen stable isotopes allow speleothem $\delta^{18}O$ values to track past climate and environments. Speleothem paleoclimatology is best complemented by in-depth understanding of the modern climate/ $\delta^{18}O$ relationships (Gonzalez and Lohmann, 1988; Baldini et al., 2006; Mattey et al., 2008). As these studies become more common, speleothem paleoclimate records will increasingly contribute to scientists' understanding of climate dynamics in the Earth system. Though most speleothem paleoclimate time series are not interpreted quantitatively in an absolute sense, they demonstrate the climate teleconnections between widely separated regions that

allow paleoclimatologists to infer regional to global-scale climate dynamics. This new approach to speleothem paleoclimatology emphasizes climate linkages between regions, and the internal and external forcing mechanisms, such as Milankovitch variations, thermohaline circulation, and latitudinal displacements of climatic zones (ITCZ, westerlies, etc.). In the future, speleothems are likely to contribute vastly more information on the Earth's climate system, and the strength of scientists' conclusions rests largely on our understanding of the climatic controls on $\delta^{18}O$ variations in the ocean, atmosphere, and cave systems.

References

Aggarwal, P.K., Frohlich, K., Kulkarni, K.M., Gourcy, L.L., 2004. Stable isotope evidence for moisture sources in the Asian summer monsoon under present and past climate regimes. Geophysical Research Letters 31. doi:10.1029/ 2004GL019911.

Alley, R.B., Cuffey, K.M., 2001. Oxygen- and hydrogen-isotopic ratios of water in precipitation: beyond paleothermometry. Reviews in Mineralogy and Geochemistry 43, 527–553.

Allison, G.B., 1982. The relationship between ^{18}O and deuterium in water in sand columns undergoing evaporation. Journal of Hydrology 55, 163–169.

Araguás-Araguás, L., Froehlich, K., Rozanski, K., 1998. Stable isotope composition of precipitation over southeast Asia. Journal of Geophysical Research 103, 28721–28742.

Asmerom, Y., Polyak, V., Burns, S., Rassmussen, J., 2007. Solar forcing of Holocene climate: new insights from a speleothem record, Southwestern United States. Geology (Boulder) 35, 1–4.

Augustin, L., Barbante, C., Barnes, P.R.F., Barnola, J.M., Bigler, M., Castellano, E., Cattani, O., Chappellaz, J., Dahl-Jensen, D., Delmonte, B., Dreyfus, G., Durand, G., Falourd, S., Fischer, H., Flueckiger, J., Hansson, M.E., Huybrechts, P., Jugie, G., Johnsen, S.J., Jouzel, J., Kaufmann, P., Kipfstuhl, J., Lambert, F., Lipenkov, V.Y., Littot, G.C., Longinelli, A., Lorrain, R., Maggi, V., Masson-Delmotte, V., Miller, H., Mulvaney, R., Oerlemans, J., Oerter, H., Orombelli, G., Parrenin, F., Peel, D.A., Petit, J.-R., Raynaud, D., Ritz, C., Ruth, U., Schwander, J., Siegenthaler, U., Souchez, R., Stauffer, B., Steffensen, J.P., Stenni, B., Stocker, T.F., Tabacco, I.E., Udisti, R., van de Wal, R.S.W., van den Broeke, M., Weiss, J., Wilhelms, F., Winther, J.-G., Wolff, E.W., Zucchelli, M., 2004. Eight glacial cycles from an Antarctic ice core. Nature (London) 429, 623–628.

Ayalon, A., Bar-Matthews, M., Kaufman, A., 2002. Climatic conditions during marine oxygen isotope stage 6 in the eastern Mediterranean region from the isotopic composition of speleothems of Soreq Cave, Israel. Geology (Boulder) 30, 303–306.

Ayalon, A., Bar-Matthews, M., Sass, E., 1998. Rainfall–recharge relationships within a karstic terrain in the eastern Mediterranean semi-arid region, Israel: $\delta^{18}O$ and δD characteristics. Journal of Hydrology 207, 18–31.

Baker, A., Mockler, N.J., Barnes, W.L., 1999. Fluorescence intensity variations of speleothem-forming groundwaters: implications for paleoclimate reconstruction. Water Resources Research 35, 407–413.

Baker, A., Smart, P.L., Edwards, R.L., Richards, D.A., 1993. Annual growth banding in a cave stalagmite. Nature 364, 518–520.

Baker, A., Smith, C.L., Jex, C., Fairchild, I.J., Genty, D., 2008. Annually laminated speleothems: a review. International Journal of Speleology 37, 193–206.

Baldini, J.U.L., McDermott, F., Fairchild, I.J., 2006. Spatial variability in cave drip water hydrochemistry: implications for stalagmite paleoclimate records. Chemical Geology 235, 390–404.

Baldini, J.U.L., McDermott, F., Hoffmann, D.L., Richards, D.A., Clipson, N., 2008. Very high-frequency and seasonal cave atmosphere pCO_2 variability: implications for stalagmite growth and oxygen isotope-based paleoclimate records. Earth and Planetary Science Letters 272, 118–129.

Bar-Matthews, M., Ayalon, A., Gilmour, M., Matthews, A., Hawkesworth, C.J., 2003. Sea–land oxygen isotopic relationships from planktonic foraminifera and speleothems in the Eastern Mediterranean region and their implication for paleorainfall during interglacial intervals. Geochimica Et Cosmochimica Acta 67, 3181–3199.

Bar-Matthews, M., Ayalon, A., Kaufman, A., 2000. Timing and hydrological conditions of sapropel events in the eastern Mediterranean, as evident from speleothems, Soreq Cave, Israel. Chemical Geology 169, 145–156.

Bar-Matthews, M., Ayalon, A., Kaufman, A., Wasserburg, G.J., 1999. The eastern Mediterranean paleoclimate as a reflection of regional events; Soreq Cave, Israel. Earth and Planetary Science Letters 166, 85–95.

Bar-Matthews, M., Ayalon, A., Matthews, A., Sass, E., Halicz, L., 1996. Carbon and oxygen isotope study of the active water-carbonate system in a karstic Mediterranean cave: implications for paleoclimate research in semiarid regions. Geochimica et Cosmochimica Acta 60, 337–347.

Barnes, C.J., Allison, G.B., 1983. The distribution of deuterium and ^{18}O in dry soils: 1. Theory. Journal of Hydrology 60, 141–156.

Beck, W.C., Grossman, E.L., Morse, J.W., 2005. Experimental studies of oxygen isotope fractionation in the carbonic acid system at 15°, 25°, and 40 °C. Geochimica et Cosmochimica Acta 69, 3493–3503.

Blisniuk, P.M., Stern, L.A., 2005. Stable isotope paleoaltimetry: a critical review. American Journal of Science 305, 1033–1074.

Bony, S., Risi, C., Vimeux, F., 2008. Influence of convective processes on the isotopic composition ($\delta^{18}O$ and δD) of precipitation and water vapor in the tropics: 1. Radiative–convective equilibrium and Tropical Ocean–Global Atmosphere–Coupled Ocean–Atmosphere Response Experiment (TOGA–COARE) simulations. Journal of Geophysical Research 113. doi:10.1029/2008JD009942.

Bowen, G.J., 2008. Spatial analysis of the intra-annual variation of precipitation isotope ratios and its climatological corollaries. Journal of Geophysical Research-Atmospheres 113. doi:10.1029/2007JD009295.

Bowen, G.J., Ehleringer, J.R., Chesson, L.A., Stange, E., Cerling, T.E., 2007. Stable isotope ratios of tap water in the contiguous United States. Water Resources Research 43. doi:10.1029/2006WR005186.

Bowen, G.J., Wilkinson, B., 2002. Spatial distribution of $\delta^{18}O$ in meteoric precipitation. Geology 30, 315–318.

Bradley, R.S., 1999. Paleoclimatology: Reconstructing Climates of the Quaternary. Harcourt Academic Press, San Diego.

Brockwell, P., 2002. Introduction to Time Series and Forecasting. Springer, London.

Broecker, W.S., Olson, E.A., Orr, P.C., 1960. Radiocarbon measurements and annual rings in cave formations. Nature 185, 93–94.

Burns, S.J., Fleitmann, D., Matter, A., Kramers, J., Al-Subbary, A.A., 2003. Indian Ocean climate and an absolute chronology over Dansgaard/Oeschger events 9 to 13. Science 301, 1365–1367.

Burns, S.J., Fleitmann, D., Mudelsee, M., Neff, U., Matter, A., Mangini, A., 2002. A 780-year annually resolved record of Indian Ocean monsoon precipitation from a speleothem from South Oman. Journal of Geophysical Research D: Atmospheres 107. doi:10.1029/2001JD001281.

Came, R.E., Eiler, J.M., Veizer, J., Azmy, K., Brand, U., Weidman, C.R., 2007. Coupling of surface temperatures and atmospheric CO_2 concentrations during the Palaeozoic era. Nature 449, 198–201.

Carrasco, F., Andreo, B., Linan, C., Mudry, J., 2006. Contribution of stable isotopes to the understanding of the unsaturated zone of a carbonate aquifer (Nerja Cave, southern Spain). Comptes Rendus Geoscience 338, 1203–1212.

Celle-Jeanton, H., Travi, Y., Blavoux, B., 2001. Isotopic typology of the precipitation in the Western Mediterranean region at three different time scales. Geophysical Research Letters 28, 1215–1218.

Chacko, T., Deines, P., 2008. Theoretical calculation of oxygen isotope fractionation factors in carbonate systems. Geochimica et Cosmochimica Acta 72, 3642–3660.

Charles, C.D., Rind, D., Jouzel, J., Koster, R.D., Fairbanks, R.G., 1994. Glacial–interglacial changes in moisture sources for Greenland – influences on the ice core record of climate. Science 263, 508–511.

Cheng, H., Edwards, R.L., Wang, Y., Kong, X., Ming, Y., Kelly, M.J., Wang, X., Gallup, C.D., Liu, W., 2006. A penultimate glacial monsoon record from Hulu Cave and two-phase glacial terminations. Geology (Boulder) 34, 217–220.

Chiang, J.C.H., Biasutti, M., Battisti, D.S., 2003. Sensitivity of the Atlantic Intertropical Convergence Zone to Last Glacial Maximum boundary conditions. Paleoceanography 18. doi:10.1029/2003PA000916.

Clark, I., Fritz, P., 1997. Environmental Isotopes in Hydrology. Lewis Publishers, New York.

Clark, I.D., Lauriol, B., 1992. Kinetic enrichment of stable isotopes in cryogenic calcites. Chemical Geology 102, 217–228.

Cobb, K.M., Adkins, J.F., Partin, J.W., Clark, B., 2007. Regional-scale climate influences on temporal variation of rainwater and cave dripwater oxygen isotopes in northern Borneo. Earth and Planetary Science Letters 263, 207–220.

Cole, J.E., Rind, D., Webb, R.S., Jouzel, J., Healy, R., 1999. Climatic controls on interannual variability of precipitation $\delta^{18}O$: simulated influence of temperature, precipitation amount, and vapor source region. Journal of Geophysical Research – Atmospheres 104, 14223–14235.

Coplen, T.B., 1995a. Discontinuance of SMOW and PDB. Nature 375, 285.

Coplen, T.B., 1995b. New IUPAC guidelines for the reporting of stable hydrogen, carbon, and oxygen isotope-ratio data. Journal of Research of the National Institute of Standards and Technology 100, 285.

Coplen, T.B., 1996. New guidelines for reporting stable hydrogen, carbon, and oxygen isotope-ratio data. Geochimica et Cosmochimica Acta 60, 3359–3360.

Coplen, T.B., 2007. Calibration of the calcite-water oxygen-isotope geothermometer at Devils Hole, Nevada, a natural laboratory. Geochimica et Cosmochimica Acta 71, 3948–3957.

Coplen, T.B., Kendall, C., Hopple, J., 1983. Comparison of stable isotope reference samples. Nature 302, 236–238.

Craig, H., 1957. Isotopic standards for carbon and oxygen and correction factors for mass-spectrometric analysis of carbon dioxide. Geochimica et Cosmochimica Acta 12, 133–149.

Craig, H., Gordon, L.I., 1965. Deuterium and oxygen 18 variations in the ocean and the marine atmosphere. In: Tongiorgi, E. (Ed.), Stable Isotopes in Oceanographic Studies and Paleotemperatures. Consiglio Nazionale delle Ricerche Laboratoria di Geologia Nucleare – Pisa, Spoleto, pp. 9–130.

Cruz, F.W., Burns, S.J., Karmann, I., Sharp, W.D., Vuille, M., Cardoso, A.O., Ferrari, J.A., Silva Dias, P.L., Viana, O., 2005a. Insolation-driven changes in atmospheric circulation over the past 116,000 years in subtropical Brazil. Nature 434, 63–66.

Cruz, F.W., Karmann, I., Viana, O., Burns, S.J., Ferrari, J.A., Vuille, M., Sial, A.N., Moreira, M.Z., 2005b. Stable isotope study of cave percolation waters in subtropical Brazil: implications for paleoclimate inferences from speleothems. Chemical Geology 220, 245–262.

Cruz, J.F.W., Burns, S.J., Karmann, I., Sharp, W.D., Vuille, M., 2006. Reconstruction of regional atmospheric circulation features during the late Pleistocene in subtropical Brazil from oxygen isotope composition of speleothems. Earth and Planetary Science Letters 248, 495–507.

Dansgaard, W., 1954. The O18-abundance in fresh water. Geochimica et Cosmochimica Acta 6, 241–260.

Dansgaard, W., 1964. Stable isotopes in precipitation. Tellus 16, 438–468.

Dansgaard, W., Johnsen, S.J., Clausen, H.B., Dahl-Jensen, D., Gundestrup, N.S., Hammer, C.U., Hvidberg, C.S., Steffensen, J.P., Sveinbjornsdottir, A.E., Jouzel, J., Bond, G., 1993. Evidence for general instability of past climate from a 250-kyr ice-core record. Nature (London) 364, 218–220.

Darling, W.G., 2004. Hydrological factors in the interpretation of stable isotopic proxy data present and past: a European perspective. Quaternary Science Reviews 23, 743–770.

Dennis, P.F., Rowe, P.J., Atkinson, T.C., 2001. The recovery and isotopic measurement of water from fluid inclusions in speleothems. Geochimica et Cosmochimica Acta 65, 871–884.

Denniston, R.F., Gonzalez, L.A., Asmerom, Y., Baker, R.G., Reagan, M.K., Bettis, E.A., 1999. Evidence for increased cool season moisture during the middle Holocene. Geology 27, 815–818.

Denton, G.H., Alley, R.B., Comer, G.C., Broecker, W.S., 2005. The role of seasonality in abrupt climate change. Quaternary Science Reviews 24, 1159–1182.

Dettman, D.L., Lohmann, K.C., 1995. Microsampling carbonates for stable-isotope and minor element analysis – physical separation of samples on a 20 micrometer scale. Journal of Sedimentary Research Section A - Sedimentary Petrology and Processes 65, 566–569.

Dincer, T., Payne, B.R., 1971. An environmental isotope study of the south-western karst region of Turkey. Journal of Hydrology 14, 233–258.

Dorale, J.A., Edwards, R.L., Ito, E., Gonzalez, L.A., 1998. Climate and vegetation history of the midcontinent from 75 to 25 ka: a speleothem record from Crevice Cave, Missouri, USA. Science 282, 1871–1874.

Drysdale, R.N., Zanchetta, G., Hellstrom, J.C., Fallick, A.E., Zhao, J.X., 2005. Stalagmite evidence for the onset of the Last Interglacial in southern Europe at $129 +/- 1$ ka: Geophysical Research Letters 32 (24), doi:10.1029/2005GL024658.

Dreybrodt, W., 2008. Evolution of the isotopic composition of carbon and oxygen in a calcite precipitating H_2O–CO_2–$CaCO_3$ solution and the related isotopic composition of calcite in stalagmites. Geochimica et Cosmochimica Acta 72, 4712–4724.

Duplessy, J.C., Labeyrie, J., Lalou, C., Nguyen, H.V., 1970. Continental climatic variations between 130,000 and 90,000 years BP. Nature (London) 226, 631–633.

Dykoski, C.A., Edwards, R.L., Cheng, H., Yuan, D., Cai, Y., Zhang, M., Lin, Y., Qing, J., An, Z., Revenaugh, J., 2005. A high-resolution, absolute-dated Holocene and deglacial Asian monsoon record from Dongge Cave, China. Earth and Planetary Science Letters 233, 71–86.

Edwards, R.L., Chen, J.H., Wasserburg, G.J., 1987. ^{238}U–^{234}U–^{230}Th–^{232}Th Systematics and the precise measurement of time over the past 5,00,000 years. Earth and Planetary Science Letters 81, 175–192.

Eiler, J.M., 2007. "Clumped-isotope" geochemistry—the study of naturally-occurring, multiply-substituted isotopologues. Earth and Planetary Science Letters 262, 309–327.

Emiliani, C., 1971. Last interglacial – paleotemperatures and chronology. Science 171, 571–573.

Epstein, S., Buchsbaum, R., Lowenstam, H.A., Urey, H.C., 1953. Revised carbonate–water isotopic temperature scale. Geological Society of America Bulletin 64, 1315–1325.

Even, H., Carmi, I., Magaritz, M., Gerson, R., 1986. Timing the transport of water through the upper vadose zone in a karstic system above a cave in Israel. Earth Surface Processes and Landforms 11, 181–191.

Fairchild, I., Baker, A., Borsato, A., Frisia, S., Hinton, R., McDermott, F., Tooth, A., 2001. Annual to sub-annual resolution of multiple trace-element trends in speleothems. Journal of the Geological Society 158, 831–841.

Fairchild, I.J., Smith, C.L., Baker, A., Fuller, L., Spötl, C., Mattey, D., McDermott, F., 2006. Modification and preservation of environmental signals in speleothems. Earth-Science Reviews 75, 105–153.

Fantidis, J., Ehhalt, D.H., 1970. Variations of the carbon and oxygen isotopic composition in stalagmites and stalactites: evidence of non-equilibrium isotopic fractionation. Earth and Planetary Science Letters 10, 136–144.

Faure, G., Mensing, T.M., 2005. Isotopes: Principles and Applications. Wiley, Hoboken.

Fetter, C.W., 1994. Applied Hydrogeology. Prentice-Hall, Englewood Cliffs.

Finch, A.A., Shaw, P.A., Weedon, G.P., Holmgren, K., 2001. Trace element variation in speleothem aragonite: potential for palaeoenvironmental reconstruction. Earth and Planetary Science Letters 186, 255–267.

Fischer, M.J., Treble, P.C., 2008. Calibrating climate-$\delta^{18}O$ regression models for the interpretation of high-resolution speleothem $\delta^{18}O$ time series. Journal of Geophysical Research 113. doi:10.1029/2007JD009694.

Fleitmann, D., Burns, S.J., Mudelsee, M., Neff, U., Kramers, J., Mangini, A., Matter, A., 2003. Holocene forcing of the Indian monsoon recorded in a stalagmite from southern Oman. Science 300, 1737–1739.

Fleitmann, D., Burns, S.J., Neff, U., Mudelsee, M., Mangini, A., Matter, A., 2004. Palaeoclimatic interpretation of high-resolution oxygen isotope profiles derived from annually laminated speleothems from southern Oman. Quaternary Science Reviews 23, 935–945.

Fontes, J.C., Yousfi, M., Allison, G.B., 1986. Estimation of long-term, diffuse groundwater discharge in the northern Sahara using stable isotope profiles in soil water. Journal of Hydrology 86, 315–327.

Fornaca-Rinaldi, G., Panichi, C., Tongiorgi, E., 1968. Some causes of the variation in the isotopic composition of carbon and oxygen in cave concretions. Earth and Planetary Science Letters 4, 321–324.

Foster, L.C., Andersson, C., Høie, H., Allison, N., Finch, A.A., Johansen, T., 2008. Effects of micromilling on δ^{18}O in biogenic aragonite. Geochemistry, Geophysics, Geosystems 9. doi:10.1029/2007GC001911.

Frappier, A., Sahagian, D., Gonzalez, L.A., Carpenter, S.J., 2002. El Niño events recorded by stalagmite carbon isotopes. Science 298, 565.

Frappier, A.B., Sahagian, D., Carpenter, S.J., Gonzalez, L.A., Frappier, B.R., 2007. Stalagmite stable isotope record of recent tropical cyclone events. Geology 35, 111–114.

Fricke, H.C., O'Neill, J.R., 1999. The correlation between ^{18}O/^{16}O ratios of meteoric water and surface temperature: its use in investigating terrestrial climate change over geologic time. Earth and Planetary Science Letters 170, 181–196.

Friedman, I., Harris, J.M., Smith, G.I., Johnson, C.A., 2002. Stable isotope composition of waters in the Great Basin, United States – 1. Air–mass trajectories. Journal of Geophysical Research-Atmospheres 107. doi:10.1029/2001JD000565.

Frisia, S., Borsato, A., Fairchild, I.J., McDermott, F., 2000. Calcite fabrics, growth mechanisms, and environments of formation in speleothems from the Italian Alps and southwestern Ireland. Journal of Sedimentary Research 70, 1183–1196.

Frisia, S., Borsato, A., Fairchild, I.J., McDermott, F., Selmo, E.M., 2002. Aragonite–calcite relationships in speleothems (Grotte De Clamouse, France): environment, fabrics, and carbonate geochemistry. Journal of Sedimentary Research 72, 687–699.

Frisia, S., Borsato, A., Spotl, C., Villa, I.M., Cucchi, F., 2005. Climate variability in the SE Alps of Italy over the past 17 000 years reconstructed from a stalagmite record. Boreas 34, 445–455.

Frot, E., van Wesemael, B., Vandenschrick, G., Souchez, R., Benet, A.S., 2007. Origin and type of rainfall for recharge of a karstic aquifer in the western Mediterranean: a case study from the Sierra de Gador-Campo de Dalias (southeast Spain). Hydrological Processes 21, 359–368.

Frumkin, A., Ford, D.C., Schwarcz, H.P., 1999. Continental oxygen isotopic record of the last 170,000 years in Jerusalem. Quaternary Research 51, 317–327.

Gascoyne, M., 1992. Palaeoclimate determination from cave calcite deposits. Quaternary Science Reviews 11, 609–632.

Gat, J.R., 1996. Oxygen and hydrogen isotopes in the hydrologic cycle. Annual Review of Earth and Planetary Sciences 24, 225–262.

Gat, J.R., Bowser, C.J., Kendall, C., 1994. The Contribution of evaporation from the Great-Lakes to the continental atmosphere – estimate based on stable-isotope data. Geophysical Research Letters 21, 557–560.

Gat, J.R., Matsui, E., 1991. Atmospheric water balance in the Amazon basin: an isotopic evapotranspiration model. Journal of Geophysical Research 96, 13179–13188.

Genty, D., Plagnes, V., Causse, C., Cattani, O., Stievenard, M., Falourd, S., Blamart, D., Ouahdi, R., Van-Exter, S., 2002. Fossil water in large stalagmite voids as a tool for paleoprecipitation stable isotope composition reconstitution and paleo-temperature calculation. Chemical Geology 184, 83–95.

Genty, D., Quinif, Y., 1996. Annually laminated sequences in the internal structure of some Belgian stalagmites: importance for paleoclimatology. Journal of Sedimentary Research 66, 275–288.

Genty, D., Vokal, B., Obelic, B., Massault, M., 1998. Bomb ^{14}C time history recorded in two modern stalagmites: importance for soil organic matter dynamics and bomb ^{14}C distribution over continents. Earth and Planetary Science Letters 160, 795–809.

Ghosh, P., Adkins, J., Affek, H., Balta, B., Guo, W.F., Schauble, E.A., Schrag, D., Eller, J.M., 2006a. ^{13}C–^{18}O bonds in carbonate minerals: a new kind of paleothermometer. Geochimica Et Cosmochimica Acta 70, 1439–1456.

Ghosh, P., Garzione, C.N., Eiler, J.M., 2006b. Rapid uplift of the Altiplano revealed through ^{13}C–^{18}O bonds in paleosol carbonates. Science 311, 511–515.

Gillieson, D., 1996. Caves: Processes, Development, Management. Blackwell, Malden, MA.

Gonfiantini, R., 1978. Standards for stable isotope measurements in natural compounds. Nature 271, 534–536.

Gonfiantini, R., 1986. Environmental isotopes in lake studies. In: Fritz, P., Fontes, J.-C. (Eds.), Handbook of Environmental Isotope Geochemistry. Elsevier, Amsterdam, pp. 113–168.

Gonfiantini, R., Roche, M.-A., Olivry, J.-C., Fontes, J.-C., Zuppi, G.M., 2001. The altitude effect on the isotopic composition of tropical rains. Chemical Geology 181, 147–167.

Gonzalez, L.A., Lohmann, K.C., 1988. Controls on mineralogy and composition of spelean carbonates: Carlsbad Caverns, New Mexico. In: James, N.P., Choquette, P.W. (Eds.), Paleokarst, pp. 81–101.

Graham, N.E., Barnett, T.P., 1987. Sea surface temperature, surface wind divergence, and convection over tropical oceans. Science 238, 657–659.

Grootes, P.M., 1993. Interpreting continental oxygen isotope records. In: Swart, P.K., Lohmann, K.L., McKenzie, J., Savin, S. (Eds.), Climate Change in Continental Isotopic Records. American Geophysical Union, Washington, DC, pp. 37–46.

Grossman, E.L., Ku, T.L., 1986. Oxygen and carbon isotope fractionation in biogenic aragonite – temperature effects. Chemical Geology 59, 59–74.

Harmon, R.S., 1979. An isotopic study of groundwater seepage in the central Kentucky karst. Water Resources Research 15, 476–480.

Hastenrath, S., 2002. The Intertropical Convergence Zone of the eastern Pacific revisited. International Journal of Climatology 22, 347–356.

Hemming, S.R., 2004. Heinrich events: massive late Pleistocene detritus layers of the North Atlantic and their global climate imprint. Reviews of Geophysics 42, RG1005.1–RG1005.43.

Hendy, C.H., 1971. The isotopic geochemistry of speleothems. 1. The calculation of the effects of different modes of formation on the isotopic composition of speleothems and their applicability as paleoclimatic indicators. Geochimica et Cosmochimica Acta 35, 801–824.

Hendy, C.H., Wilson, A.T., 1968. Palaeoclimatic data from speleothems. Nature (London) 219, 48–51.

Herbert, T.D., Schuffert, J.D., Andreasen, D., Heusser, L., Lyle, M., Mix, A., Ravelo, A.C., Stott, L.D., Heguera, J.C., 2002. The California current, Devils Hole, and Pleistocene climate – response. Science 296, 7a.

Herbert, T.D., Schuffert, J.D., Andreasen, D., Heusser, L., Lyle, M., Mix, A., Ravelo, A.C., Stott, L.D., Herguera, J.C., 2001. Collapse of the California current during glacial maxima linked to climate change on land. Science 293, 71–76.

Holland, H.D., Kirsipu, T.V., Huebner, J.S., Oxburgh, U.M., 1964. On some aspects of the chemical evolution of cave waters. Journal of Geology 72, 36–67.

Holmgren, K., Karlen, W., Shaw, P.A., 1995. Paleoclimatic significance of the stable isotopic composition and petrology of a late pleistocene stalagmite from Botswana. Quaternary Research 43, 320–328.

Horita, J., Clayton, R.N., 2007. Comment on the studies of oxygen isotope fractionation between calcium carbonates and water at low temperatures by Zhou and Zheng (2003, 2005). Geochimica et Cosmochimica Acta 71, 3131–3135.

Hurrell, J.W., Kushnir, Y., Ottersen, G., Visbeck, M., 2003. The North Atlantic oscillation: climatic significance and environmental impacts. In: Geophysical Monograph 134. American Geophysical Union, Washington, DC, p. 279.

IAEA/WMO, 2004. Global Network of Isotopes in Precipitation. The GNIP Database. Available from: <http://isohis.iaea.org>.

Ingraham, N.L., Chapman, J.B., Hess, J.W., 1990. Stable isotopes in cave pool systems – Carlsbad-Cavern, New-Mexico, USA. Chemical Geology 86, 65–74.

Ingraham, N.L., Taylor, B.E., 1991. Light stable isotope systematics of large-scale hydrologic regimes in California and Nevada. Water Resources Research 27, 77–90.

Johnsen, S.J., Clausen, H.B., Dansgaard, W., Fuhrer, K., Gundestrup, N., Hammer, C.U., Iversen, P., Jouzel, J., Stauffer, B., Steffensen, J.P., 1992. Irregular glacial interstadials recorded in a New Greenland ice core. Nature 359, 311–313.

Johnsen, S.J., DahlJensen, D., Gundestrup, N., Steffensen, J.P., Clausen, H.B., Miller, H., Masson-Delmotte, V., Sveinbjornsdottir, A.E., White, J., 2001. Oxygen isotope and palaeotemperature records from six Greenland ice-core stations: Camp Century, Dye-3, GRIP, GISP2, Renland and NorthGRIP. Journal of Quaternary Science 16, 299–307.

Johnson, K.R., Ingram, B.L., 2004. Spatial and temporal variability in the stable isotope systematics of modern precipitation in China: implications for paleoclimate reconstructions. Earth and Planetary Science Letters 220, 365–377.

Jones, I.C., Banner, J.L., Humphrey, J.D., 2000. Estimating recharge in a tropical karst aquifer. Water Resources Research 36, 1289–1299.

Jouzel, J., Alley, R.B., Cuffey, K.M., Dansgaard, W., Grootes, P.M., Hoffmann, G., Johnsen, S.J., Koster, R.D., Peel, D., Shuman, C.A., Stievenard, M., White, J.W.C., Hammer, C.U., Mayewski, P.A., Peel, D., Stuiver, M., 1997. Validity of the temperature reconstruction from water isotopes in ice cores. Journal of Geophysical Research 102, 26471–26487.

Kelly, M.J., Edwards, R.L., Cheng, H., Yuan, D., Cai, Y., Zhang, M., Lin, Y., An, Z., 2006. High resolution characterization of the Asian monsoon between 146,000 and 99,000 years B.P. from Dongge Cave, China and global correlation of events surrounding termination II. Palaeogeography Palaeoclimatology Palaeoecology 236, 20–38.

Kendall, C., Coplen, T.B., 2001. Distribution of ^{18}O and deuterium in river waters across the United States. Hydrological Processes 15, 1363–1393.

Kim, S.-T., O'Neil, J.R., 1997. Equilibrium and nonequilibrium oxygen isotope effects in synthetic carbonates. Geochimica et Cosmochimica Acta 61, 3461–3475.

Kim, S.-T., O'Neil, J.R., 2005. Comment on "An experimental study of oxygen isotope fractionation between inorganically precipitated aragonite and water at low temperatures" by G.-T. Zhou and Y.-F. Zheng. Geochimica et Cosmochimica Acta 69, 3195–3197.

Kim, S.-T., O'Neil, J.R., Hillaire-Marcel, C., Mucci, A., 2007. Oxygen isotope fractionation between synthetic aragonite and water: influence of temperature and Mg^{2+} concentration. Geochimica et Cosmochimica Acta 71, 4704–4715.

Klein, R.T., Lohmann, K.C., 1995. Isotopic homogeneity among nonequivalent sectors of calcite. Geology 23, 633–636.

Klimchouk, A., 2000. The formation of epikarst and its role in vadose speleogenesis. In: Klimchouk, A., Ford, D.C., Palmer, A.N., Dreybrodt, W. (Eds.), Speleogenesis: Evolution of Karst Aquifers. National Speleological Society, Huntsville, pp. 91–99.

Kluge, T., Marx, T., Scholz, D., Niggemann, S., Mangini, A., Aeschbach-Hertig, W., 2008. A new tool for palaeoclimate reconstruction: noble gas temperatures from fluid inclusions in speleothems. Earth and Planetary Science Letters 269, 408–415.

Kohn, M.J., Welker, J.M., 2005. On the temperature correlation of δ^{18}O in modern precipitation. Earth and Planetary Science Letters 231, 87–96.

Kolodny, Y., Bar-Matthews, M., Ayalon, A., McKeegan, K.D., 2003. A high spatial resolution δ^{18}O profile of a speleothem using an ion-microprobe. Chemical Geology 197, 21–28.

Kong, X., Wang, Y., Edwards, R.L., Cheng, H., Wang, X., 2005. The altitude effect on oxygen isotope composition of stalagmite. Abstracts with Programs – Geological Society of America 37, 13.

Koster, R.D., Devalpine, D.P., Jouzel, J., 1993. Continental water recycling and $H_2^{18}O$ concentrations. Geophysical Research Letters 20, 2215–2218.

Lacelle, D., 2007. Environmental setting, (micro)morphologies and stable C–O isotope composition of cold climate carbonate precipitates – a review and evaluation of their potential as paleoclimatic proxies. Quaternary Science Reviews 26, 1670–1689.

Lachniet, M.S., Asmerom, Y., Burns, S., Patterson, W.P., Polyak, V., Seltzer, G.O., 2004a. Tropical response to the 8200 yr cold event? Speleothem isotopes indicate a weakened early Holocene monsoon in Costa Rica. Geology 32, 957–960.

Lachniet, M.S., Burns, S.J., Piperno, D.R., Asmerom, Y., Polyak, V.J., Moy, C.M., Christenson, K., 2004b. A 1500 year El Niño/Southern oscillation and rainfall history for the Isthmus of Panama from speleothem calcite. Journal of Geophysical Research D: Atmospheres 109. doi:10.1029/2004JD004694.

Lachniet, M.S., Patterson, W.P., 2002. Stable isotope values of Costa Rican surface waters. Journal of Hydrology 260, 135–150.

Lachniet, M.S., Patterson, W.P., 2006. Use of correlation and multiple stepwise regression to evaluate the climatic controls on the stable isotope values of Panamanian surface waters. Journal of Hydrology 324, 115–140.

Lachniet, M.S., Patterson, W.P., Burns, S.J., Asmerom, Y., Polyak, V.J., 2007. Caribbean and Pacific moisture sources on the Isthmus of Panama revealed from stalagmite and surface water $\delta^{18}O$ gradients. Geophysical Research Letters 34. doi:10.1029/2006GL028469.

Lawrence, J.R., 1998. Isotopic spikes from tropical cyclones in surface waters: opportunities in hydrology and paleoclimatology. Chemical Geology 144, 153–160.

Lawrence, J.R., Gedzelman, S.D., 1996. Low stable isotope ratios of tropical cyclone rains. Geophysical Research Letters 23, 527–530.

Lawrence, J.R., Gedzelman, S.D., White, J.W.C., Smiley, D., Lazov, P., 1982. Storm trajectories in Eastern-United-States D/H isotopic composition of precipitation. Nature 296, 638–640.

Lea, D.W., Martin, P.A., Pak, D.K., Spero, H.J., 2002. Reconstructing a 350 ky history of sea level using planktonic Mg/Ca and oxygen isotope records from a Cocos Ridge core. Quaternary Science Reviews 21, 283–293.

Lee, J.-E., Fung, I., DePaolo, D.J., Otto-Bliesner, B., 2008. Water isotopes during the Last Glacial Maximum: new general circulation model calculations. Journal of Geophysical Research 113. doi:10.1029/2008JD009859.

Leffler, A.J., Enquist, B.J., 2002. Carbon isotope composition of tree leaves from Guanacaste, Costa Rica: comparison across tropical forests and tree life history. Journal of Tropical Ecology 18, 151–159.

LeGrande, A.N., Schmidt, G.A., 2006. Global gridded data set of the oxygen isotopic composition in seawater. Geophysical Research Letters 33. doi:10.1029/2006GL026011.

Liu, B., Phillips, F., Hoines, S., Campbell, A.R., Sharma, P., 1995. Water movement in desert soil traced by hydrogen and oxygen isotopes, chloride, and ^{36}Cl, southern Arizona. Journal of Hydrology 168, 91–110.

Long, A.J., Putnam, L.D., 2004. Linear model describing three components of flow in karst aquifers using ^{18}O data. Journal of Hydrology 296, 254–270.

Longinelli, A., Edmond, J.M., 1983. Isotope geochemistry of the Amazon basin: a reconnaissance. Journal of Geophysical Research 88, 3703–3717.

Machavaram, M.V., Krishnamurthy, R.V., 1995. Earth surface evaporative process: a case study from the Great Lakes region of the United States based on deuterium excess in precipitation. Geochimica et Cosmochimica Acta 59, 4179–4283.

Mangini, A., Spötl, C., Verdes, P., 2005. Reconstruction of temperature in the Central Alps during the past 2000 yr from a $\delta^{18}O$ stalagmite record. Earth and Planetary Science Letters 235, 741–751.

Mattey, D., Lowry, D., Duffet, J., Fisher, R., Hodge, E., Frisia, S., 2008. A 53 year seasonally resolved oxygen and carbon isotope record from a modern Gibraltar speleothem: reconstructed drip water and relationship to local precipitation. Earth and Planetary Science Letters 269, 80–95.

Matthews, A., Ayalon, A., Bar-Matthews, M., 2000. D/H ratios of fluid inclusions of Soreq cave (Israel) speleothems as a guide to the Eastern Mediterranean Meteoric Line relationships in the last 120 ky. Chemical Geology 166, 183–191.

McDermott, F., 2004. Palaeo-climate reconstruction from stable isotope variations in speleothems: a review. Quaternary Science Reviews 23, 901–918.

McDermott, F., Frisia, S., Huang, Y., Longinelli, A., Spiro, B., Heaton, T.H.E., Hawkesworth, C.J., Borsato, A., Keppens, E., Fairchild, I.J., van der Borg, K., Verheyden, S., Selmo, E., 1999. Holocene climate variability in Europe: evidence from $\delta^{18}O$, textural and extension-rate variations in three speleothems. Quaternary Science Reviews 18, 1021–1038.

McDonald, J., Drysdale, R., Hill, D., Chisari, R., Wong, H., 2007. The hydrochemical response of cave drip waters to sub-annual and inter-annual climate variability, Wombeyan Caves, SE Australia. Chemical Geology 244, 605–623.

McMillan, E.A., Fairchild, I.J., Frisia, S., Borsato, A., McDermott, F., 2005. Annual trace element cycles in calcite–aragonite speleothems: evidence of drought in the western Mediterranean 1200–1100 yr BP. Journal of Quaternary Science 20, 423–433.

Merlivat, L., Jouzel, J., 1979. Global climatic interpretation of the deuterium–oxygen-18 relationship for precipitation. Journal of Geophysical Research-Oceans and Atmospheres 84, 5029–5033.

Michaelis, J., Usdowski, E., Menschel, G., 1985. Partitioning of ^{13}C and ^{12}C on the degassing of CO_2 and the precipitation of calcite – Rayleigh-type fractionation and a kinetic-model. American Journal of Science 285, 318–327.

Mickler, P.J., Banner, J.L., Stern, L., Asmerom, Y., Edwards, R.L., Ito, E., 2004. Stable isotope variations in modern tropical speleothems: evaluating equilibrium vs. kinetic isotope effects. Geochimica et Cosmochimica Acta 68, 4381.

Mickler, P.J., Stern, L.A., Banner, J.L., 2006. Large kinetic isotope effects in modern speleothems. Geological Society of America Bulletin 118, 65–81.

Moreira, M.Z., Sternberg, L.D.L., Martinelli, L.A., Victoria, R.L., Barbosa, E.M., Bonates, L.C.M., Nepstad, D.C., 1997. Contribution of transpiration to forest ambient vapour based on isotopic measurements. Global Change Biology 3, 439–450.

Neff, U., Burns, S.J., Mangini, A., Mudelsee, M., Fleitmann, D., Matter, A., 2001. Strong coherence between solar variability and the monsoon in Oman between 9 and 6 kyr ago. Nature (London) 411, 290–293.

Njitchoua, R., Sigha-Nkamdjou, L., Dever, L., Marlin, C., Sighomnou, D., Nia, P., 1999. Variations of the stable isotopic compositions of rainfall events from the Cameroon rain forest, Central Africa. Journal of Hydrology 223, 17–26.

Patterson, W.P., Smith, G.R., Lohmann, K.C., 1993. Continental paleothermometry and seasonality using the isotopic composition of aragonitic otoliths of freshwater fishes. Geophysical Monograph 78, 191–202.

Perrin, K., Jeannin, P.Y., Zwahlen, F., 2003. Epikarst storage in a karst aquifer: a conceptual model based on isotopic data, Milandre test site, Switzerland. Journal of Hydrology 279, 106–124.

Poage, M.A., Chamberlain, C.P., 2001. Empirical relationships between elevation and the stable isotope composition of precipitation and surface waters: considerations for studies of paleoelevation change. American Journal of Science 301, 1–15.

Polyak, V.J., Asmerom, Y., 2001. Late Holocene climate and cultural changes in the southwestern United States. Science 294, 148–151.

Poulson, T.L., White, W.B., 1969. The cave environment. Science 165, 971–981.

Quade, J., Cerling, T.E., Bowman, J.R., 1989. Systematic variations in the carbon and oxygen isotopic composition of pedogenic carbonate along elevation transects in the Southern Great-Basin, United-States. Geological Society of America Bulletin 101, 464–475.

Quinn, T.M., Taylor, F.W., Crowley, T.J., Link, S.M., 1996. Evaluation of sampling resolution in coral stable isotope records: a case study using records from New Caledonia and Tarawa. Paleoceanography 11, 529–542.

Railsback, L.B., Brook, G.A., Chen, J., Kalin, R., Fleisher, C.J., 1994. Environmental controls on the petrology of a Late Holocene speleothem from Botswana with annual layers of aragonite and calcite. Journal of Sedimentary Research Section A – Sedimentary Petrology and Processes 64, 147–155.

Read, R.G., 1977. Microclimate as background environment for ecological-studies of insects in a tropical forest. Journal of Applied Meteorology 16, 1282–1291.

Richards, D., Dorale, J., 2003. Uranium-series chronology and environmental applications of speleothems. Reviews in Mineralogy 52, 407–460.

Risi, C., Bony, S., Vimeux, F., 2008. Influence of convective processes on the isotopic composition ($\delta^{18}O$ and δD) of precipitation and water vapor in the tropics: 2. Physical interpretation of the amount effect. Journal of Geophysical Research 113. doi:10.1029/2008JD009943.

Roberts, M.S., Smart, P.L., Baker, A., 1998. Annual trace element variations in a Holocene speleothem. Earth and Planetary Science Letters 154, 237–246.

Romanov, D., Kaufmann, G., Dreybrodt, W., 2008. $\delta^{13}C$ profiles along growth layers of stalagmites: comparing theoretical and experimental results. Geochimica et Cosmochimica Acta 72, 438–448.

Ropelewski, C.F., Halpert, M.S., 1987. Global and regional scale precipitation patterns associated with the El-Nino southern oscillation. Monthly Weather Review 115, 1606–1626.

Rowley, D.B., Pierrehumbert, R.T., Currie, B.S., 2001. A new approach to stable isotope-based paleoaltimetry: implications for paleoaltimetry and paleohypsometry of the High Himalaya since the Late Miocene. Earth and Planetary Science Letters 188, 253–268.

Rozanski, K., Araguás-Araguás, L., Gonfiantini, R., 1993. Isotopic patterns in modern global precipitation. In: Swart, P.K., Lohmann, K.L., McKenzie, J., Savin, S. (Eds.), Climate Change in Continental Isotopic Records. American Geophysical Union, Washington, DC, pp. 1–37.

Salati, E., Dall'ollio, A., Matsui, E., Gat, J.R., 1979. Recycling of water in the Amazon basin: an isotopic study. Water Resources Research 15, 1250–1258.

Schmidt, G.A., LeGrande, A.N., Hoffmann, G., 2007. Water isotope expressions of intrinsic and forced variability in a coupled ocean–atmosphere model. Journal of Geophysical Research-Atmospheres 112. doi:10.1029/2006JD007781.

Schrag, D.P., Adkins, J.F., McIntyre, K., Alexander, J.L., Hodell, D.A., Charles, C.D., McManus, J.F., 2002. The oxygen isotopic composition of seawater during the last glacial maximum. Quaternary Science Reviews 21, 331–342.

Schrag, D.P., Hampt, G., Murray, D.W., 1996. Pore fluid constraints on the temperature and oxygen isotopic composition of the glacial ocean. Science 272, 1930–1932.

Schwarcz, H.P., 1986. Geochronology and isotopic geochemistry of speleothems. In: Handbook of Environmental Isotope Geochemistry. pp. 271–303.

Sengupta, S., Sarkar, A., 2006. Stable isotope evidence of dual (Arabian Sea and Bay of Bengal) vapour sources in monsoonal precipitation over north India. Earth and Planetary Science Letters 250, 511–521.

Severinghaus, J.P., Brook, E.J., 1999. Abrupt climate change at the end of the last glacial period inferred from trapped air in polar ice. Science 286, 930–934.

Shackleton, N.J., Fairbanks, R.G., Chiu, T.C., Parrenin, F., 2004. Absolute calibration of the Greenland time scale: implications for Antarctic time scales and for $\Delta^{14}C$. Quaternary Science Reviews 23, 1513–1522.

Shakun, J.D., Burns, S.J., Fleitmann, D., Kramers, J., Matter, A., Al-Subary, A., 2007. A high-resolution, absolute-dated deglacial speleothem record of Indian Ocean climate from Socotra Island, Yemen. Earth and Planetary Science Letters 259, 442–456.

Sharp, Z., 2007. Principles of Stable Isotope Geochemistry. Pearson Prentice Hall, Upper Saddle River, NJ.

Shopov, Y.Y., Ford, D.C., Schwarcz, H.P., 1994. Luminescent microbanding in speleothems: high-resolution chronology and paleoclimate. Geology (Boulder) 22, 407–410.

Shuster, E.T., White, W.B., 1972. Source areas and climatic effects in carbonate groundwaters determined by saturation indices and carbon dioxide pressures. Water Resources Research 8, 1067–1073.

Spötl, C., Mangini, A., 2002. Stalagmite from the Austrian Alps reveals Dansgaard–Oeschger events during isotope stage 3: implications for the absolute chronology of Greenland ice cores. Earth and Planetary Science Letters 203, 507–518.

Spötl, C., Mangini, A., Richards, D.A., 2006. Chronology and paleoenvironment of marine isotope stage 3 from two high-elevation speleothems, Austrian Alps. Quaternary Science Reviews 25, 1127–1136.

Spötl, C., Mattey, D., 2006. Stable isotope microsampling of speleothems for palaeoenvironmental studies: a comparison of microdrill, micromill and laser ablation techniques. Chemical Geology 235, 48–58.

Strong, M., Sharp, Z.D., Gutzler, D.S., 2007. Diagnosing moisture transport using D/H ratios of water vapor. Geophysical Research Letters 34. doi:10.1029/2006GL028307.

Stuiver, M., Grootes, P.M., 2000. GISP2 oxygen isotope ratios. Quaternary Research 53, 277–283.

Sturm, C., Vimeux, F., Krinner, G., 2008. Intraseasonal variability in South America recorded in stable water isotopes. Journal of Geophysical Research 112. doi:10.1029/2007JD008298.

Stute, M., Schlosser, P., Clark, J.F., Broecker, W.S., 1992. Paleotemperatures in the Southwestern United-States derived from noble-gases in ground-water. Science 256, 1000–1003.

Talma, A.S., Vogel, J.C., 1992. Late Quaternary paleotemperatures derived from a speleothem from Cango Caves, Cape Province, South Africa. Quaternary Research 37, 203–213.

Tang, K., Feng, X., 2001. The effect of soil hydrology on the oxygen and hydrogen isotopic compositions of plants' source water. Earth and Planetary Science Letters 185, 355–367.

Tarutani, T., Clayton, R.N., Mayeda, T.K., 1969. The effect of polymorphism and magnesium substitution on oxygen isotope fractionation between calcium carbonate and water. Geochimica et Cosmochimica Acta 33, 987–996.

Taupin, J.D., Coudrain-Ribstein, A., Gallaire, R., Zuppi, G.M., Filly, A., 2000. Rainfall characteristics (δ^{18}O, δ^2H, H, ΔT, and ΔH_r) in western Africa: regional scale and influence of irrigated areas. Journal of Geophysical Research-Atmospheres 105, 11911–11924.

Treble, P.C., Budd, W.F., Hope, P.K., Rustomji, P.K., 2005a. Synoptic-scale climate patterns associated with rainfall δ^{18}O in southern Australia. Journal of Hydrology 302, 270–282.

Treble, P.C., Chappell, J., Gagan, M.K., McKeegan, K.D., Harrison, T.M., 2005b. In situ measurement of seasonal δ^{18}O variations and analysis of isotopic trends in a modern speleothem from southwest Australia. Earth and Planetary Science Letters 233, 17–32.

Treble, P.C., Schmitt, A.K., Edwards, R.L., McKeegan, K.D., Harrison, T.M., Grove, M., Cheng, H., Wang, Y.J., 2007. High-resolution secondary ionization mass spectrometry (SIMS) δ^{18}O analyses of Hulu Cave speleothem at the time of Heinrich event 1. Chemical Geology 238, 197–212.

van Breukelen, M.R., Vonhof, H.B., Hellstrom, J.C., Wester, W.C.G., Kroon, D., 2008. Fossil dripwater in stalagmites reveals Holocene temperature and rainfall variation in Amazonia. Earth and Planetary Science Letters 275, 54–60.

Vandenschrick, G., van Wesemael, B., Frot, E., Pulido-Bosch, A., Molina, L., Stievenard, M., Souchez, R., 2002. Using stable isotope analysis (δD–δ^{18}O) to characterise the regional hydrology of the Sierra de Gador, south east Spain. Journal of Hydrology 265, 43–55.

Vimeux, F., Gallaire, R., Bony, S., Hoffmann, G., Chiang, J.C.H., 2005. What are the climate controls on δD in precipitation in the Zongo Valley (Bolivia)? Implications for the Illimani ice core interpretation. Earth and Planetary Science Letters 240, 205–220.

Vuille, M., Werner, M., 2005. Stable isotopes in precipitation recording South American summer monsoon and ENSO variability: observations and model results. Climate Dynamics 25, 401–413.

Vuille, M., Werner, M., Bradley, R.S., Keimig, F., 2005. Stable isotopes in precipitation in the Asian monsoon region. Journal of Geophysical Research – Atmospheres 110. doi:10.1029/2005JD006022.

Wagner, J.D., Cole, J.E., Cole, J.E., Beck, J.W., Patchett, P.J., Henderson, G.M., 2005. Abrupt millennial climate change in the Arizona desert inferred from a speleothem isotopic record. In: American Geophysical Union Fall Meeting Abstracts, San Francisco, CA. p. 262.

Wang, X., Auler, A.S., Edwards, R.L., Cheng, H., Cristalli, P.S., Smart, P.L., Richards, D.A., Shen, C.-C., 2004. Wet periods in northeastern Brazil over the past 210 kyr linked to distant climate anomalies. Nature (London) 432, 740–743.

Wang, X., Auler, A.S., Edwards, R.L., Cheng, H., Ito, E., Solheid, M., 2006. Interhemispheric anti-phasing of rainfall during the last glacial period. Quaternary Science Reviews 25, 3391–3403.

Wang, Y.J., Cheng, H., Edwards, R.L., An, Z.S., Wu, J.Y., Shen, C.C., Dorale, J.A., 2001. A high-resolution absolute-dated Late Pleistocene monsoon record from Hulu Cave, China. Science 294, 2345–2348.

Werner, M., Heimann, M., Hoffmann, G., 2001. Isotopic composition and origin of polar precipitation in present and glacial climate simulations. Tellus Series B: Chemical and Physical Meteorology 53, 53–71.

Wiedner, E., Scholz, D., Mangini, A., Polag, D., Mühlinghaus, C., Segl, M., 2008. Investigation of the stable isotope fractionation in speleothems with laboratory experiments. Quaternary International 187, 15–24.

Williams, P.W., 2008. The role of the epikarst in karst and cave hydrogeology: a review. International Journal of Speleology 37, 1–10.

Williams, P.W., Marshall, A., Ford, D.C., Jenkinson, A.V., 1999. Palaeoclimatic interpretation of stable isotope data from Holocene speleothems of the Waitomo district, North Island, New Zealand. The Holocene 9, 649–657.

Winograd, I.J., 2002. The California current, Devils Hole, and Pleistocene climate. Science 296, 7a.

Winograd, I.J., Coplen, T.B., Landwehr, J.M., Riggs, A.C., Ludwig, K.R., Szabo, B.J., Kolesar, P.T., Revesz, K.M., 1992. Continuous 500,000-year climate record from vein calcite in Devils Hole, Nevada. Science 258, 255–260.

Winograd, I.J., Landwehr, J.M., Coplen, T.B., Sharp, W.D., Riggs, A.C., Ludwig, K.R., Kolesar, P.T., 2006. Devils Hole, Nevada, δ^{18}O record extended to the mid-Holocene. Quaternary Research 66, 202–212.

Winograd, I.J., Riggs, A.C., Coplen, T.B., 1998. The relative contributions of summer and cool-season precipitation to groundwater recharge, Spring Mountains, Nevada, USA. Hydrogeology Journal 6, 77–93.

Wurster, C.M., Patterson, W.P., Cheatham, M.M., 1999. Advances in micromilling techniques: a new apparatus for acquiring high-resolution oxygen and carbon stable isotope values and major/minor elemental ratios from accretionary carbonate. Computers & Geoscience 25, 1159–1166.

Yamada, M., Ohsawa, S., Matsuoka, H., Watanabe, Y., Brahmantyo, B., Maryunani, K.A., Tagami, T., Kitaoka, K., Takemura, K., Yoden, S., 2008. Derivation of travel time of limestone cave drip water using tritium/^{3}He dating method. Geophysical Research Letters 35. doi:10.1029/2008GL033237.

Yang, W., Lowenstein, T.K., Krouse, H.R., Spencer, R.J., Ku, T.-L., 2005. A 200,000 year δ^{18}O record of closed-basin lacustrine calcite, Death Valley, California. Chemical Geology 216, 99–111.

Yonge, C.J., Ford, D.C., Gray, J., Schwarcz, H.P., 1985. Stable isotope studies of cave seepage water. Chemical Geology 58, 97–105.

Yuan, D., Cheng, H., Edwards, R.L., Dykoski, C.A., Kelly, M.J., Zhang, M., Qing, J., Lin, Y., Wang, Y., Wu, J., Dorale, J.A., An, Z., Cai, Y., 2004. Timing, duration, and transitions of the last interglacial Asian monsoon. Science 304, 575–578.

Zaucker, F., Broecker, W.S., 1992. The influence of atmospheric moisture transport on the fresh water balance of the Atlantic drainage basin: general circulation model simulations and observations. Journal of Geophysical Research 97, 2765–2773.

Zheng, Y.-F., Zhou, G.-T., 2007. Response to the comment by J. Horita and R.N. Clayton on "The studies of oxygen isotope fractionation between calcium carbonates and water at low temperatures". Geochimica et Cosmochimica Acta 71, 3136–3143.

Zhou, G.T., Zheng, Y.F., 2003. An experimental study of oxygen isotope fractionation between inorganically precipitated aragonite and water at low temperatures. Geochimica et Cosmochimica Acta 67, 387–399.